FEDERAL UNIVERSITY OF TECHNOLOGY - PARANÁ

MASTER'S PROGRAM IN MATERIALS SCIENCE AND ENGINEERING

ARMANDO ALFREDO ESCRIBÁ FLORES

MWCNT composite with polymer matrix applied to pollutants retention

LONDRINA

2021

ARMANDO ALFREDO ESCRIBÁ FLORES

MWCNT COMPOSITE WITH POLYMER MATRIX APPLIED TO POLLUTANTS RETENTION

-

COMPOSTO DE MWCNTS EM MATRIZ POLIMÉRICA COM APLICAÇÃO NA RETENÇÃO DE CONTAMINANTES

Dissertation presented to the Post-Graduation Program in Materials Science and Engineering, from the Federal University of Technology of Paraná.

Concentration area: Materials for engineering and technology purposes

Research area: Nano-structured materials

Supervisor: Prof. Carlos Eduardo Cava[1]

LONDRINA

2021

ARMANDO ALFREDO ESCRIBA FLORES

MWCNT COMPOSITE WITH POLYMER MATRIX APPLIED TO POLLUTANTS RETENTION

Trabalho de pesquisa de mestrado apresentado como requisito para obtenção do título de Mestre Em Ciência E Engenharia De Materiais da Universidade Tecnológica Federal do Paraná (UTFPR). Área de concentração: Materiais Para Aplicação Em Engenharia E Tecnologia.

Data de aprovação: 06 de Setembro de 2021

Prof Carlos Eduardo Cava, Doutorado - Universidade Tecnológica Federal do Paraná

Prof Eduardo Guilherme Cividini Neiva, Doutorado - Universidade Regional de Blumenau (Furb)

Prof Edvani Curti Muniz, - Universidade Tecnológica Federal do Paraná

Documento gerado pelo Sistema Acadêmico da UTFPR a partir dos dados da Ata de Defesa em 06/09/2021.

To my parents Alfredo and Noemi who always gave me their love and support.

ACKNOWLEDGMENT

Never consider study as an obligation, but as the opportunity to
penetrate the beautiful and wonderful world of knowledge.

(Albert Einstein)

Escribá, Armando A. **MWCNT COMPOSITE WITH POLYMER MATRIX APPLIED TO POLLUTANTS RETENTION**. 2021. 61 ST. DISSERTATION POST-GRADUATION PROGRAM IN MATERIALS SCIENCE AND ENGINEERING, FROM THE FEDERAL TECHNOLOGICAL UNIVERSITY OF PARANÁ, LONDRINA, 2021.

ABSTRACT

Pollutants present in water or air can directly affect the human health and at the same time present a negative effect over the entire ecosystem. The development of materials or methods for rejection of contaminants can create mechanisms to mitigate water and air pollution. Absorption and filtration by membrane process are frequently used in the rejection of some pollutants presents in the water or air. The surface area, permeability, flux, are some important properties evaluated for filter mediums. To produce new advanced materials for pollution rejection, electrospinning is a promising methodology which allows the formation of polymeric fibers. These fibers can be conformed to a membrane with a high surface area, good mechanical stability and interconnected porous. These properties make the membrane produced by an electrospinning technique present the potential capacity to deal with some contaminants present in the water or air. The membranes production by electrospinning is very sensitive to many parameters and the choice of the polymeric matrix is crucial to obtain the membrane with the desired properties. PVC (Poly(vinyl chloride)) is one of the most used polymers in the industry, the versatility of PVC allows the formation of electrospun fibers. The incorporation of nanomaterials over the electrospun matrix, such as mult-wall carbon nanotubes (MWCNTs), makes possible to improve the membrane properties such as surface area, enhancing its rejection capacity. At this work, it was developed fibers with a polymer blend PVC/PVP conformed by electrospinning. The obtained fibers with an average diameter of 240 nm also was possible to incorporate MWCNTS over the matrix showing an interesting morphology over the membrane.

Keywords: Electrospinning; PVC/PVP; MWCNTs; filtration.

RESUMO

Os contaminantes na água e no ar podem afetar diretamente a saúde humana, ao mesmo tempo podem presentar efeitos negativos sobre o ecossistema. No desenvolvimento de materiais e métodos para a retenção de contaminantes permitem a criação de mecanismos para a mitigação de contaminação na água e no ar. Adsorção e filtragem por meio de processo de membrana são frequentemente usadas na retenção de contaminantes na água e no ar. A área superficial, permeabilidade, fluxo são algumas propriedades importantes avaliadas para meios filtrantes. Para produzir novos materiais avançados na retenção de contaminantes, *electrospinning* é uma metodologia promissória que permite a criação de fibras poliméricas. Estas fibras podem formar uma membrana com alta área superficial, boa estabilidade mecânica e poros interconectados. Estas propriedades fazem que uma membrana composta por *electrospinning* presente uma capacidade potencial para lidar com alguns contaminantes presentes na água ou no ar. A produção de membranas por *electrospinning* é muito sensível a vários parâmetros e a seleção da matriz polimérica é crucial para obter uma membrana com propriedades específicas. PVC (PoliCloreto de Vinil) é um dos mais usados polímeros na indústria e a versatilidade do PVC permite a formação de fibras eletrofiadas. A incorporação de nanomatérias sobre uma matriz produzida com *electrospinning* com nanotubos de carbono (MWCNTs), possibilita melhoras nas propriedades da membrana, como aumento da área superficial, e uma melhoria na capacidade de remoção. Neste trabalho foi desenvolvida uma membrana polimérica composta por PVC/PVP com o método electrospinning. As fibras obtidas por esta metodologia apresentaram um diâmetro de 240 nm e foi possível incorporar MWCNTs sobre a superfície da matriz apresentando uma morfologia interessante.

Keywords: Electrospinning; PVC/PVP; MWCNTs; Filtragem.

FIGURES INDEX

TABLE INDEX

LIST OF ABBREVIATIONS

DMAC	Dimethylacetamide
DSC	Differential Scanning Calorimetry
DTGA	Differential Thermogravimetry
IR-Spectroscopy	Infra-Red spectroscopy
MWCNTs	Multi-Walled Carbon Nanotubes
PVC	Poly (vinyl chloride)
PVP	Poly(vinylpyrrolidone)
SEM	Scanning Electron Microscopy
TGA	Thermogravimetry

INDEX

1 INTRODUCTION

Contaminants present in water and air are public health and environmental concerns (HU et al., 2020; HUTTON, 2013; WWDR, 2015). As a result of unsustainable development, industrialization, economic and population growth, the quality of water and air are compromised by many types of pollutants (WWDR, 2015). Many diseases can be associated with the presence of pollutants in the water or the air. The emerging contaminants present in the water refers the pollutants that were not present in the past and are present now in a wide of sources of water, pharmaceuticals, chemicals, heavy metals, etc are some of them (GOGOI et al., 2018; MOHAMMADI et al., 2020). At the same time, the amounts of atmospheric particulate matter are worrying in various cities around the world, the high concentration of particulate matter is associated with respiratory diseases (BRAUER et al., 2021; BROOK et al., 2010; RILES; BROOK, 2011).

The develop of new materials or methods in the rejection of contaminants present in the water or air could be a good strategy to deal with the emerging pollutants present in the water or to reject atmospheric pollution. Materials with high surface area, good chemical and mechanical stability and good interaction with the contaminants could be suitable for be used in filtering process, adsorption, or absorption process. With the development of materials with that characteristic will be possibly create systems for keep environments controlled of some contaminants.

Electrospinning is a promising technology and widely studied by its interesting properties. The possibility of synthesizing micro and nanofiber allows creates a layer with high surface area, interconnected porous, and good mechanical properties. Some researchers have shown interesting results in the rejection of emerging pollutants in membrane process (PARK et al., 2018; SHEN et al., 2020; ULBRICHT, 2006; WANG et al., 2020; ZHANG et al., 2020b). In this study, it is considered a synthesis and characterization of a PVC/PVP and MWCNTS electrospun nanocomposite for adsorptive and membrane process purpose. Electrospinning is a technique with allows the formation of micro or nanofiber, the fibers form membranes that can be used in a wide of areas, such as optoelectronic devices, absorption, filtering, medicine, water treatment etc.

1.1 JUSTIFICATION

Water is an essential liquid for the existence of life. The unsustainable development has created huge pressure under the regular sources of freshwater (WWDR, 2015). Some contaminants that were not present in the past are found today in the regular sources of fresh water and the regular methods as flocculation-coagulation, coloration, ozonation, are not designed to deal with the emerging pollutants or are expensive and time-consuming (WEN et al., 2013a).

Some technologies such as membrane process exhibit interesting properties with potential capacity to deal with some emerging contaminants; high selectivity, does not need an extra precursor for work, does not generate a secondary pollutant exist a categorization in terms of selectivity (MULDER, 1996). Under the methodology of electrospinning is possible to generate a membrane confirmed by micro or nanofibers. Some advantages confirmed by this methodology is that the membrane has a high flux, antifouling properties, interconnected porous (SUJA et al., 2017). The advanced nanomaterials open another window of possibilities in the process of water treatment. The unique properties of the nanomaterials such as high surface area, superior mechanical properties, physicochemical properties made the advanced nanomaterials suitable to incorporate in a membrane such as a composite.

Under the methodology of electrospinning is possible to develop a composite confirmed by a polymeric electrospun membrane and with different techniques of deposition is possible to incorporate a nanomaterial over the surface of the fibers and enhance its properties. PVC is one of the most used polymers in the world and the versatility of that polymer allows the formation of fibers by electrospinning method (QUOC PHAM et al., 2021; WYPYCH, 2016b), with the incorporation of MWCNTS is possible to increase its performance in the membrane process of adsorption process.

1.2 OBJETIVES

1.2.1 General objective

Synthesis and characterization of an electrospun nanocomposite membrane conformed by PVC/PVP/MWCNTs for removal contaminants in the water.

1.2.2 Specific objectives

- Synthesis a membrane conformed by electrospun nanofiber of PVC/PVP blend
- Analyze the hydrophobic nature of the composite by its water angle contact outcome
- Make a deposition of MWCNTs by casting, self-assembled and spray over the surface of the fibers
- Analyze the morphology of the electrospun PVC/PVP fibers and, the dispersion of the MWCNTs over the surface of the fibers with a scanning electron microscope (SEM)
- Evaluate the glass transition temperature of the composite by differential scanning calorimetry (DSC)
- Determine the thermal stability of the composite by Thermal gravimetry (TGA)
- Determine the presence of both polymers PVC and PVP by infrared spectroscopy.
- Analyze the rheological properties of the blend PVC/PVP dissolved in DAMC for the best results obtained in the formation of fiber

2 THEORICAL FRAMEWORK

2.1 WATER FOR A SUSTAINABLE WORLD

Sustainable development consists of to use the natural resources to cover the present necessities without compromising the future generations, granting the balance between economic growth, environmental and social well-being. The unsustainable development has created high pressure over the quality and availability of the fresh water (HOUNGBO, 2018; WADA et al., 2016; WWDR, 2015). The scarcity of the water affect nearly 40% of the global population and it is projected to rise (WWDR, 2015) the economic growth, fast urbanization and industrialization had been affected by the quality of the water directly, more than 80% of wastewater is discharge in rivers, lakes or seas without any wastewater treatment and; approximately 70% of all the fresh water, obtained by rivers or aquifers is used for irrigation, and approximately the 15% is used to generate energy and the last 15% of fresh water is used by the industry and domestical consumption (WWDR, 2015).

The water is an essential liquid to maintain a life, everyone needs access to safe water in adequate quantities for cooking, personal hygiene and sanitation facilities (WWDR, 2015). The lack of water sanitation and hygiene takes a huge cost in terms of well-being, environmental and the impact is approximately reflected in terms of financial costs (WWDR, 2015). 748 millions of people don't use an improved source of water, 2.5 billion don't use a sanitation facility and an estimated of 24% of the global population is consuming water with Escherichia Coli (WWDR, 2015). The return on investment in water sanitation services has been estimated at US$5 to US$28 per dollar invested (HUTTON, 2013).

The presence of emerging contaminants in the regular sources of fresh water is a concern in terms of public health and can affect directly the ecosystems (WWDR, 2015). The emerging contaminants in the water are defined such as elements or contaminants that were not present in the past and are found today in the regular sources of fresh water. The presence of emerging contaminants in the water can create changes in the human behavior, landscape, water resources, microbial adaptation. It is possible to make a characterization of emerging pollutants,

such as pharmaceuticals, algal toxins, microorganisms, and another chemical (KUMAR; BORAH; DEVI, 2020). The majority of all the emerging contaminants came from anthropogenic sources, detecting the principal sources of emerging contaminants open a possibility to create a control of detection and removal. Table 1 shows some emerging contaminants and its principles sources.

Table 1: Relation with some contaminates found in the water, its adverse known effects, and the source.

Contaminant	Adverse effects	Source
Endocrine-disrupting compounds and personal care products	Endocrine system disruption	Wastewater
Pharmaceuticals	Unknown	Wastewater
Antibiotic resistance genes	Pathogen resistance to antibiotics	Human and animal antibiotics
Cyanotoxins	Liver and nervous system damage	Blue-green algae
Human parasites, bacteria, viruses	Infections	Wastewater
Zoonotic parasites, bacteria, viruses pathogenic to humans	Infections	Animal waste
N-nitrosodimethylamine	Carcinogenesis	by-product of wastewater chlorination
Methyltertbutylether	Toxicity	Fuel oxygenate
Alkylphenolpolyethoxylates	Toxicity	Degradation of surfactants
Fluorinated alkyl surfactants Toxicity Industrial processes	Toxicity	Industrial processes
Polybrominated diphenyl ethers	Toxicity	Flame retardants
Benzotriazoles	Toxicity	Anticorrosives, wastewater
Naphthenic acids	Toxicity	Crude oil, wastewater
New, chiral, and transformed pesticides	Toxicity, carcinogenesis	Wastewater
Disinfection by-products	Toxicity	Chlorination by-products of emerging contaminants

Source: Data recovered from (KUMAR; BORAH; DEVI, 2020).

The regular drinking water treatments such as coagulation-flocculation, sedimentation, filtration, ozone treatment, precipitation adsorption and disinfection are not designed to deal with that pollutants or are expensive and time consuming that's why those don't represent an interesting way to deal with that emerging pollutants (WEN et al., 2013b). Adsorption or membrane process are some methodologies used to reject contaminants present in the water or air, high surface area, flux, permeability, and reusability are some of the principal properties desire in membrane or adsorption process. The incorporation of advanced materials on or in a matrix could enhance or create new possibilities in the removal of contaminants in the water or air (ESCRIBÁ et al., 2021). MWCNTS are promising material for be used in a wide of areas, such as removal of contaminants, optoelectronic devices, transport of energy, composites etc. (KARIIM et al., 2020).

2.2 CARBON NANOTUBES

The structure of carbon nanotube can be understood as a graphene sheet enrolled as cylinder and it results in a tubular structure. The diameter is very close to some nanometers and the length can reach values near to 28×10^6 times its diameter. The periodicity in one direction is associated with a mono crystallinity (JAVIER; MARTÍNEZ, 2010). Figure 1 an example representation of a single and multiwalled carbon nanotubes.

Figure 1: Schematic representations of Single-walled carbon nanotube (SWCNT) and multi-walled carbon nanotube (MWCNT).
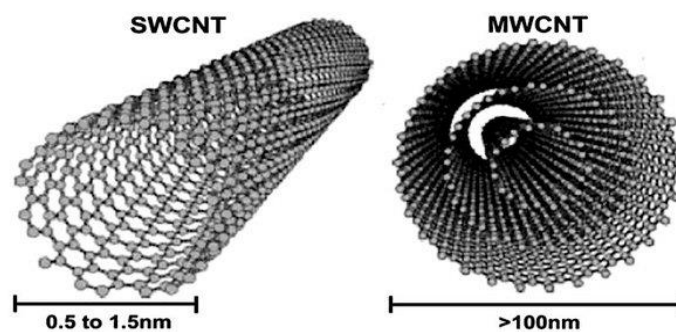
Source: Recovery from (RIBEIRO et al., 2017).

Exist some methods to produce carbon nanotubes but original method arc-discharge used by Ijima (SUMIO LIJIMA, 1991), who discovered carbon nanotubes in 1990. The equipment consists in a vacuum chamber, in a *He* atmosphere, and 2 electrodes. The electrodes are 2 bars of high purity graphite. The temperature in this chamber can rise to 3000°C that is the temperature necessary to evaporate carbon atoms. The requirements for synthetized nanotubes consist in a voltage between 20-25 V into electrodes, and the current needs to be between 50-120 A (Direct Current). The pressure of He to produce nanotubes are 0.7 atm. The process of synthesis nanotubes involves impurities that are extremely hard to remove.

Carbon nanotubes are considered the strongest materials in the nature at this point. The principal tool to analyze the mechanical properties are associated with Young'´s Modulus. Unfortunately, some variables related with its structure make measuring any variable complicated. The diameter, chirality are the principle geometrical aspects that need to be considered while measuring some properties; the literature suggest that the Young´s modulus have ranges from 270 to 950 GPa, while the tensile strength is algo high, in the ranges of 11-63 GPa.

Carbon nanotubes are very small, and the quantum effects are important and need to be considered, specific heat and thermal conductivity evidence that. Some researcher found that the thermal conductivity for an individual MWCNTs is up to 3000 W/mK. This property is very important to include in a polymer in a nanocomposite (HE et al., 2021). As the nanotubes as consider a nanomaterial its high surface area is an important property that can be useful in the rejection of contaminants in the water, its chemical stability also provides some advantages in terms of   reusability (KARIIM et al., 2020; PARREIRA et al., 2019).

The utilization of carbon nanotubes is wide, from optoelectronic devices (HUANG et al., 2021; KHAN et al., 2020; XIE; SUGIME; NODA, 2021) to wasting and drinking water treatment (ANSARI et al., 2011; CHENG et al., 2019; JAIN; JEE KANU, 2021; LUAN; TEYCHENE; HUANG, 2019), its unique properties generate wide options to be used such as reinforced materials in composites (ARRECHEA et al., 2020; DELE-AFOLABI et al., 2020; THIRUGNANASAMBANTHAM et al., 2021) or active layer in different process such adsorption or membrane process. With the

incorporation of electrospinning process, it is possible to incorporate that nanomaterial on and in the surface of the polymeric fibers.

2.3 POLY(VINYL CHLORIDE) (PVC)

It is the second thermoplastic polymer most used and produced in world at global scale PVC reach up to 35 million of ton per year surpassing the polystyrene that is the leader in the plastic industry. The properties of PVC allow wide applications in different processing conditions for develop different products used in the industry. Table 2 shows some of the principal characteristics of PVC.

Table 2: Principal physical characteristics of PVC.

PVC characteristic	Unit	Range of values
Density	g*cm^{-3}	1.45[a]
Mass average molecular weight, M_w	dalton	37,000-214,000[c]
Polydispersity, M_w/M_n	--	1.90-2.59 (suspension); 2.14-2.65 (emulsion); 2.00-2.06 (mass)[c]
Mean particle diameter	µm	100-150 Å [b]
Melting temperature, DSC	°C	103-230; 400 (syndiotactic, estimate) [c]
Young modulus	MPa	2.43-400[b]
Tensile strain	MPa	7.1-63.2[b]
Resistivity	Ω-cm	1E14[b]
Hansen solubility parameters, δD, δp, δH	Mpa$^{0.5}$	(18.82, 10.03, 3.07); (16.8, 8.9, 6.1); (18.4, 6.6, 8.0) [c]
Interaction Radius (R)	Mpa$^{0.5}$	3.5

a (AKOVALI, 2012)
b (WYPYCH, 2020a)
c (WYPYCH, 2016b)
Source: Done by the author.

Vinyl chloride is the monomer used in the conformation of PVC, Figure 2 shows the structure of the vinyl chloride.

Figure 2: Schematic representation of Vinyl chloride chemical molecule.
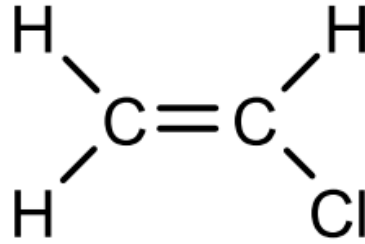
Source: Done by the author.

Vinyl chloride has low reactivity, but its radical shape is highly reactive, that's why radical polymerization is an appropriate way to produce PVC. The initiation process consists in two steps. First the initiator produces a vinyl chloride radical that react with vinyl chloride monomer forming a new radical for the process of propagation. The initiator plays an important role in the properties of the polymeric chain, can influence its molecular weight, and polymerization rate. The process of propagation consists in the incorporation of more monomers in the growing radical, as much monomer are added in the process more will be the molecular weight of the chain. The quantity of monomers needs to be controlled to avoid the defects in the polymer chains. The process of termination occurs by disproportion and combination (WYPYCH, 2020).

2.4 ELECTROSPINNING

The electrospinning method allows the formation of polymeric fibers at micro- and nanometric scale (SUJA et al., 2017). The electrospinning process consists in pumping a polymeric solution out of a syringe. A syringe pump manages the rate in which the solution is being expelled out of the syringe's needle, a positive charge is induced at the needle's tip while a negative charge is induced on the collector, this induces a jet of polymer out of the needle. The electric field is subjected at the end of the needle which contains the polymer solution. It is also helped by its surface tension, forming the Taylor cone at the end of the needle, the field induces a charge in the surface of the polymer solution, the instability creates a discharge jet of solution from the needle to the collector with a negative charge, meanwhile, the

solvents are evaporating in the journey and leaving the polymer fiber in the collector (RAHMATI et al., 2021; STACE et al., 2019).

An electrospinning apparatus is basically composed of the following items: a high voltage source, a collector, a syringe pump, a needle diameter, and polymer solution. Each of these components play an important part on the performance of the electrospun fiber, affecting its formation, morphology, and structure. In this case the diameter of the fibers and quantity of beads can be affected. Figure 3 shows a schematic representation of a regular non-commercial electrospinning apparatus and two SEM image of electrospun fibers, (1) syringe pump, (2) electrical source, (3) polymer solution, (4) jet, (5) collector. The performance of the fibers must be controlled and optimized by some internal parameters, such as voltage, feed rate, distance between the tip of the needle and the collector, diameter of the needle, polymer solvent concentration, temperature, humidity.

Figure 3: Electrospinning apparatus (A) and electrospun fibers (B, C)
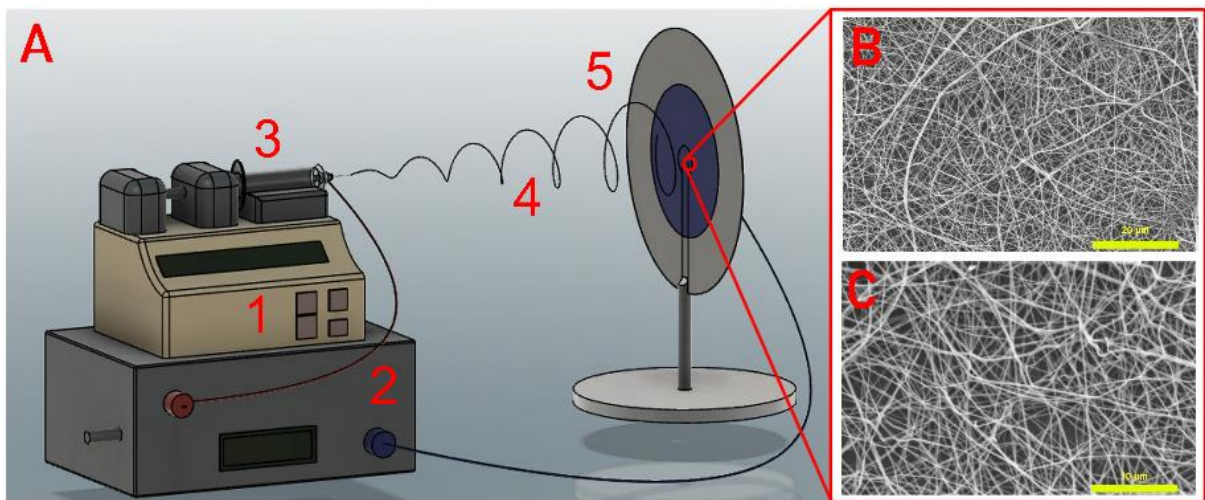
Source: Recovery from (ESCRIBÁ et al., 2021)

Caption: (A) Schematic representation of the principal elements conform the electrospinning apparatus, (1) Syringe pump, (2) electric source, (3) Solution in syringe, (4) Jet and (Collector); (B) SEM image of PVC/PVP electrospun fiber with x5000 magnification, (C) SEM image of PVC/PVP electrospun fiber with magnification x10000.

2.4.1 Internal and external parameters

Solution concentration: It is an important parameter that needs to be controlled to produce fibers free of beads and with a small diameter. The relationship sol-

vent/polymer plays an important role in the solution viscosity while increases the viscosity is evidenced in the presence of polymer chain entanglements. The entanglements stabilize the solution droplets in the tip of the needle, producing electrospun fibers-free beads. With low concentrations, the entanglements do not exist, and the jet presents instabilities showing defects in the production of the electrospun fibers, the presence of beads is evidenced with low concentrations. Meanwhile, in the presence of a very high concentration, the viscosity of the solution increases at the same time. The solvent evaporates and the production of electrospun fibers is interrupted by the needle clogging. The determination of the optimum condition depends on each case (CORRADINI et al., 2017).

Molecular weight: molecular weight is a polymer property that has a relevant effect on the rheological and electrical properties, such as dielectric strength, viscosity, and tension surface. The entanglements are associated with molecular weight. Solution with low molecular weight present small fractions of entanglements that influence the presence of beads in electrospun fibers. Meanwhile with polymers with high molecular weight the diameters of the fibers increase (CORRADINI et al., 2017).

Viscosity: The viscosity is a relevant parameter in the electrospinning process defining fibers diameter and morphology. It is difficult to obtain continuous fibers from solutions with low viscosity. While with solutions with high viscosity the formation of the jet during the electrospinning process is complicated. Considering that the viscosity is associated with the concentration solvent/polymer and molecular weight. The optimal concentration depends on the polymer used in the solution (CORRADINI et al., 2017).

 Surface tension: The surface tension is associated with the nature of solvent and the polymer concentration used in the solution. Depending on the solvent and low polymer concentration, a decrease in the surface solution occurs, the electrospun fibers can shows few or nothing or beads. With high concentrations of polymer, the surface tension increases and for control the number of beads will be necessary increase the voltage (CORRADINI et al., 2017).

Conductivity: The conductivity depends on both polymer and solvent. The use of polymers with high conductivity allows the formation of small fibers. meanwhile solutions prepared with polymers with low conductivity don't show uniformity and shows presence of beads (CORRADINI et al., 2017).

Applied voltage: Voltage is a very important parameter that needs to be controlled in the electrospinning process. A high density of positive charge can be induced in the droplet ubicated in the tip of the needle. This condition overcoming the surface tension and the formation of the jet starts. In order is increased the voltage applied the elongation of the polymer chains increases and the diameter of the fibers decreases, depending of the high values of voltages more than 15 kV commonly are evidenced high concentration of beads (CORRADINI et al., 2017).

Flow rate: It refers to the among of electric-charged solution that is ejected in the electrospinning process in a determined time. The synergic relationship between voltage and flow rate can produce fibers without beads. Low flow rates are used commonly for low volatile solvents, allowing the evaporation of solvent in the travel from the tip of the needle to the collector. Meanwhile, high flow rates are commonly used with volatile solvents. Even with volatile solvents and high flow rates the fibers can presents beads by the short dry time (CORRADINI et al., 2017).

Tip-to-collector distance: It consists of the distance between the tip of the needle to the collector. And it represents an adjustment that needs to be controlled, when the distance is too close the solution will not have enough time to evaporate the solvent, producing flat or thick fibers. while the distance is high the behavior is similar such as if the voltage applied was low (CORRADINI et al., 2017).

Diameter of the needle: The diameter needle plays an important role, the diameter of the needle governs the size of the drop of solution in the tip, considering that phenomenon it affects the surface tension, it is evident that with small diameter increases the surface tension while increases the diameter decreases the surface tension (ABUNAHEL et al., 2018) .

Humidity and temperature: the atmospheric conditions play an important role in the electrospinning process, the temperature affects some conditions such as the viscosity of the solution and solvent evaporation rate. The humidity plays an important role in the electrospinning process and morphology of the fibers. high relative humidity has a negative effect on the formation of electrospun fibers production, fiber reaches the collector before the solvent evaporates forming a fusion of fibers and beads. For polymers with hydrophobic nature, the water acts such as nonsolvent, and during the evaporation process pores are formed in the electrospun fibers. Meanwhile, with very low relative humidity in the process of evaporation, the solvents evaporate at a high rate forming thicker fibers (CORRADINI et al., 2017).

The versatility of the PVC allows the formation of electrospun fibers but unfortunately PVC is a polymer the were not significant studied by its difficult in surface functionalization (SUJA et al., 2017), the incorporation of another polymer enhance the quality of the fibers, the incorporation of PVP, PS and PAN reduces que diameter of the fibers (QUOC PHAM et al., 2021).

2.5 MEMBRANE PROCESS

The membrane process is commonly used in water treatments and it consists of four elements: two water phases, one interphase named membrane, and the force driving, which is pressure in this case (MULDER, 1996), Figure 4 shows a schematic representation of a regular membrane process. The membranes can be categorized by its pore size and pressure conduction in microfiltration, ultrafiltration, nanofiltration, reverse osmosis, and forward osmosis.

Figure 4: Schematic representation of membrane process
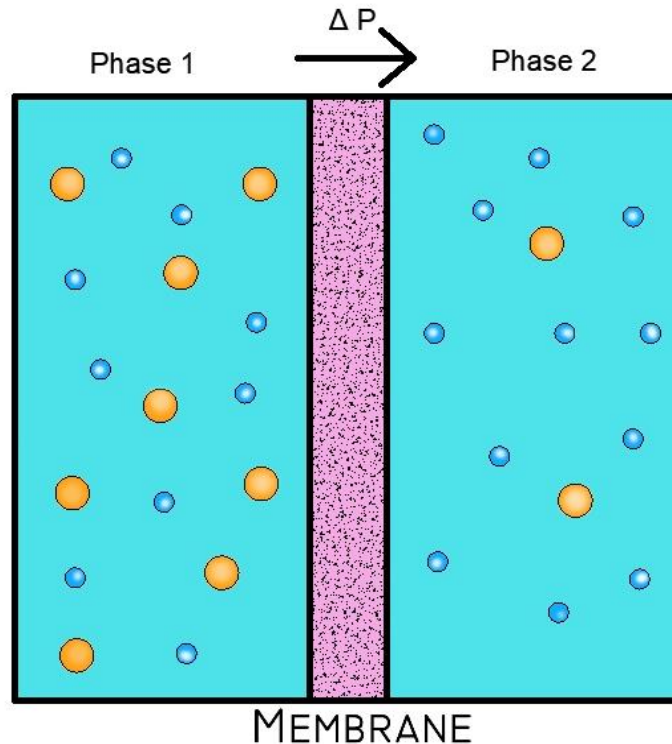
Source: Recovery from (ESCRIBÁ et al., 2021).

Caption: Schematic representation of membrane process, phase 1 with a high concentration in comparison with phase 2, the interphase is named membrane and is represented in the middle with color purple, and, in the membrane an amount of concentration is rejected. The process is governed by the pressure difference (ΔP) between phase 1 and phase 2. The small blue circles represent the particles that can easily cross the membrane and the orange circles represent the removal target of the membrane.

Microfiltration: It is probably the membrane process closer to coarse filtration. Pore size range is 0.05-10 μm, pressure driving is less than 2 bar, and sieving its principle of separation. Due to its pore size range, this membrane process is suitable to retain suspensions and emulsions (MULDER, 1996). Numerous studies have shown good performance in the rejection of some contaminants present in the water using electrospun membranes (ISLAM; MCCUTCHEON; RAHAMAN, 2017; LIU et al., 2013).

Microfiltration: It is a process between micro-filtration and nano-filtration, presenting properties close to both, such as pore size, which is between 0.05 μm (in the micro-filtration side) and 1 nm (in the nano-filtration side). It works with pressures of 1-10 bar, and sieving is its separation principle, which is the same as for micro-filtration. Ultra-filtration membrane process is frequently used to reject macro-

molecules and colloids with a few thousands of Dalton from liquid solutions (MULDER, 1996). The incorporation of the electrospinning technology in ultra-filtration process has shown interesting results (WANG et al., 2020; ZHAO et al., 2012).

Nanofiltration: It is a process employed when there is a necessity to reject low molecular weight solutes, such as inorganic salts or organic molecules, like glucose or sucrose. Solution-diffusion is the principle that governs the separation, nanofiltration works with pressures of 10-25 bar, and its pore size is less than 2 nm, nanofiltration membranes are frequently composed of more than one phase, making a composite. A high hydrodynamic resistance is needed to cover the high pressure demand (MULDER, 1996). Some interesting results have used the electrospinning process to use as intermediate layer in nanofiltration process (KAUR et al., 2011; SHEN et al., 2020).

Reverse and forward osmosis: it is technologies used in water treatments, and they are based on the same principle of osmotic pressure to operate. Figure 5 shows a scheme of an osmosis process using in desalination process. The main application in water treatment consists in desalination of brackish and seawater to produce freshwater. The quantity of salt in brackish is around 1000-5000 ppm and near to 35,000 ppm for seawater. These technologies can be utilized in other industries, such as the food industry and the metallurgic industry, to name a few (MULDER, 1996). More recently, forward osmosis (FO) is a process that allows the separation process with less energy consumption. FO works similarly to regular osmosis process, but the osmotic pressure is managed with the incorporation of controlled solutes for the former (PARK et al., 2018; YADAV et al., 2020).

The utilization of electrospinning membranes as intermediate layer in forward osmosis and reverse osmosis have demonstrated interesting results in the removal of salts, the hydrophilic nature and mechanical properties of the polymer used in the electrospun layer plays an important role in the performance of the membrane (PARK et al., 2018; YIP et al., 2010).

Figure 5: Schematic representation of the regular Osmosis, reverse osmosis and forward osmosis process.
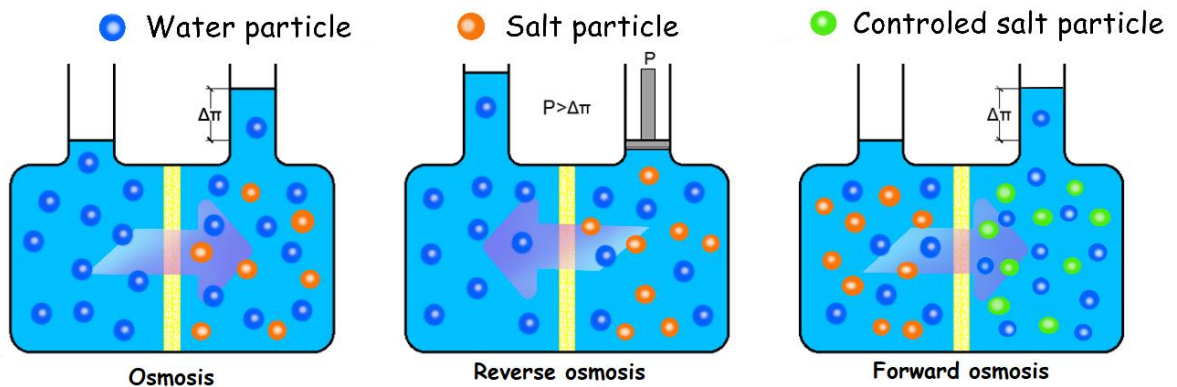
Source: Recovery from (ESCRIBÁ et al., 2021).

Caption: Osmosis: That process consist in the movement of the liquid with less concentration to the site with more concentration, (blue circles represent water particles and orange circles represent particles of NaCl) the purple arrow shows the movement of the particles. In reverse osmosis, an external pressure is applied in the site more concentrated, the purple arrow shows the movement of the particles. In forward Osmosis a controlled charge of salt (green circles) is added with the intention of increase the concentration in one of the sites without the particle target and the phenomenon of diffusion happens such as regular osmosis process the purple arrow shows the movement of the particles.

3 CHARACTERIZATION METHODS

3.1 SCANNING ELECTRON MICROSCOPE

The scanning electron microscopy is a technique used to know the morphology of the sample, the principal difference between the optic microscopy and electron microscopy is that the optic microscopy works with light, and the electronic microscope uses an electron beam over the sample and produces a magnified image; the Broglie wavelength about 100,000 times shorter than visible light, electron microscopy can have a high definition near to 0.05 nm and magnification up to 10,000,000x. The process of how the SEM works is similar with a optic microscopy, the phenomenon is reflected and transmitted light in optic microscopy are analogous to the detector in order to collect the photons, secondary and back scattered electrons in SEM (INKSON, 2016).

The imaging signals came from low energy secondary electrons and back-scattered electrons. Two dedicated detectors named, *Everhart-Thornley* (ETD), *and through the lens (TLD),* both can detect secondary electrons and backscattered electrons, usually for high resolution is used TLD and for lower resolution imaging ETD is used. The information which came from the secondary electrons could be translated as the topography in the surface of the sample, and backscattered electrons signals provide information about the composition of the sample, another interesting tool that is incorporated in modern SEM is X-ray diffraction (INKSON, 2016) .

The electron beam can be generated in two ways: field emission or a thermionic emission. Field emission consists in applying a high potential electrical field near the fine filament which makes the ejection of electrons direct towards the sample; from thermionic emission, a high current is passed through the conducting filament (INKSON, 2016).

The electron beam is generated by electron gun, and the electron beam penetrates the sample and generates the emission of electrons with different energies spectra. As well as another electromagnetic radiations, the emission of this

electrons contains some information about the sample´s surface, topography, crystallographic formation, chemical composition and another properties (INKSON, 2016).

The electron beam needs to be created under high vacuum to collimate the beam and prevent premature electron scattering; the electron beam is aligned to the sample and the beam trough the column of electromagnetic lens, as shown in the Figure 6. The lens practically coils which collimates, condenses, and focus the electron beam, to the sample. In addition to the last lens, the SEM has also two extra coils which can deflect the beam and allows the raster scanning on the surface sample for 2D imaging (INKSON, 2016).

The sample chamber works with Ultra high vacuum (UHV), near to 10^{-6} Torr. That environment in ultra-high vacuum can create conflicts with the nature of the material to be imaged, samples with high vapor pressure such a liquids and biological samples can loss water and another volatiles in vacuum (INKSON, 2016).

Figure 6: Schematic representation of the principal elements that conform Electron Scanning Microscope.
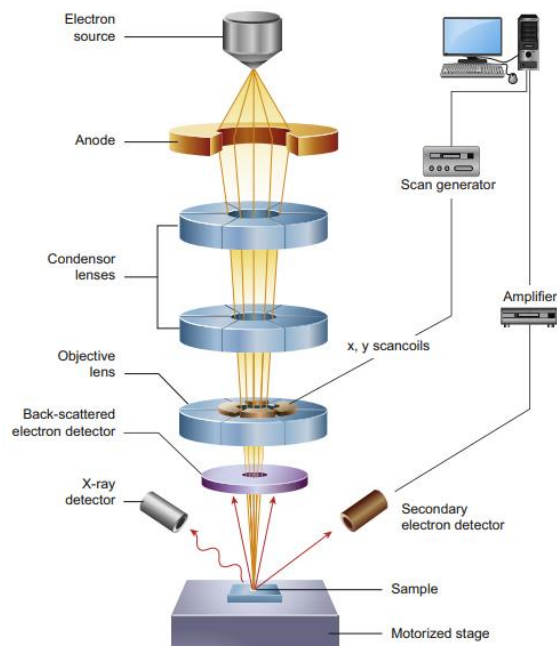
Source: Recovery from (INKSON, 2016).

3.1.1 Sample preparation

Scanning electron microscopes has the capacity to magnify a sample up to values near to 150,000x with-quality resolution and intense detail. The type of samples that SEM can works include desiccated and conductive, desiccated, and non-conductive. Desiccated and conductive samples are easily imagen without an extra preparation. Desiccated and non-conductive samples need to be coated with a conductive layer protecting the sample for the heating and improving the image quality. For non-conductive samples it is necessary to use to use a sputter coater to coat the sample with a thin layer of metal highly conduct such as gold. A sputter coater uses argon ions to beat off the atoms of the highly conductive material to coat the surface of the sample(NGUYEN; HARBISON, 2017). Gold, gold-palatinum, gold-palladium, chromium and iridium are the most metals used for coating samples in SEM, the thickness of the coating is between 2-5 nm, samples with thin coating can has a non-uniform distribution of the metal and the electrons beans can damage the sample. When the thickness of the sample is high some details in the surface of the sample are not evidenced (NGUYEN; HARBISON, 2017).

3.2 IR SPECTROSCOPY

The principles pf spectrophotometric is a function of how the light interacts with the matter Figure 7 The main aspects to take into consideration are the phenomenon of transmission, where the light can pass through the matter; and the phenomenon of reflection, where the light is reflected by the sample surface. In these two processes, the sample can absorb some part of the incident energy, and it is possible to obtain information from these phenomena according to the sample.

Figure 7: Light interactions with the matter in assistance of photospectrometry technics.
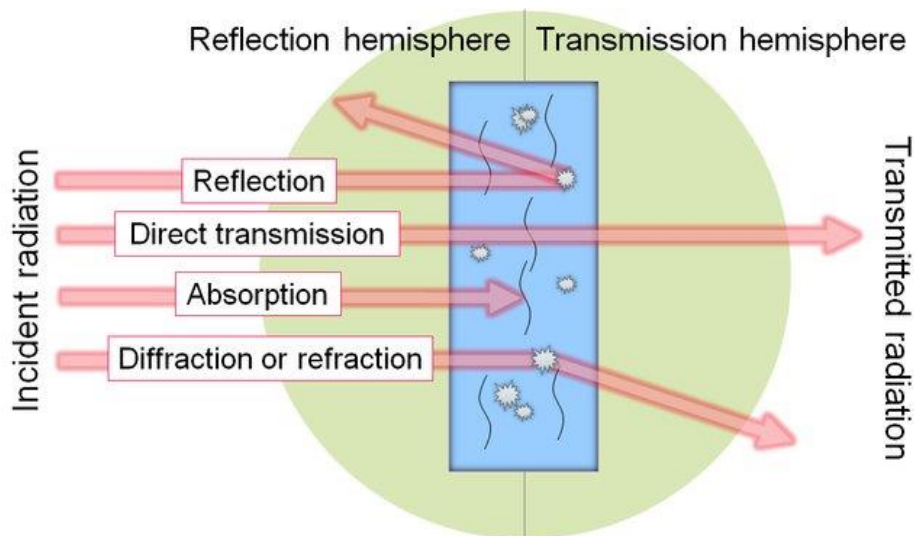
Source: Recovery from (HYLL, 2016).

The process of absorption of energy can generate movements in the molecules (displacement or rotation), or it can cause vibrations in specific groups and some electrons can be in an excited state. The process of IR spectroscopy, monitoring the vibrations of the molecules under IR light; the vibration can be symmetric or asymmetric. To induce these vibrations, the energy of the electromagnetic radiation must be an exact match as the ground state and in an excited state, also, it will change the dipole moment. These 2 conditions are called resonance conditions for unpolarized light (WEN et al., 2013b).

The IR spectrometer produces the IR light over the range wavelength and monitors the vibration of molecules. The process basically consists of IR light source, an interferometer to generate the wave numbers, and a detector to record the signal. The interferometer is probably the most important part, and it consists of a fixed mirror, moving mirrors, and a beam splitter. The beam-splitter splits the IR beam and recombines to produce different IR wavelengths. The mirrors are used to deflect the IR beam. The laser acts as a reference of data collector, the detector recovers the different signals as an interferogram, which then is Fuorier-Transformated to result in a single beam spectrum. The background state of the IR light interacts with the transition of sample to obtain the spectrum of the sample. The combination of light by the fixed mirror and the moving mirror gives several signals in the IR spectrum and

the detector can analyze all these combinations at the same time (WEN et al., 2013b).

3.3 WATER ANGLE CONTACT

The surface wetting properties of a membrane plays an important role under the point of view that affects its performance in terms of rejection, flux, and fouling characteristics. The analysis of liquid on solid can give us some interesting information about the surface properties of a membrane; in general terms wettability and hydrophobicity has a significant influence in terms of flux, foiling and self-life and efficacy. Those properties can be associated with the measure of water angle contact of a pure drop over the surface membrane. The material composition governs the interactions with water molecules that influence the wettability. The determination of a water contact angle for low values will term it to be hydrophilic nature and for high values it will be hydrophobic nature (AGRAWAL et al., 2017; HEBBAR; ISLOOR; ISMAIL, 2017). Figure 8 shows a schematic representation of a water angle contact.

Figure 8: Schematic presentation of hydrophobic and hydrophilic substrate with a drop of water.
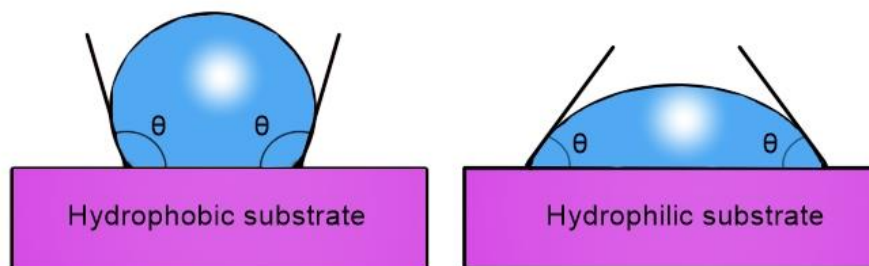
Source: Done by the author.

Caption: Schematic presentation of hydrophobic and hydrophilic substrate with a drop of water. Hydrophobic substrates show values more than 90° degrees such as is shown in the left scheme. The hydrophilic substrates show vales less than 90° values such as is shown un the right scheme.

The measure of water angle contact depends on some parameter that influence the behavior of the drop of water over the surface of the substrate. The physicochemical properties of such as heterogeneity, surface roughness, particle size and particle shape have been detected as the four properties that can have

more influence in the measure of water angle contact. The roughness of any material will have a significant influence in the macroscopic measure of angle. The process of measuring could influence moistening, spreading, and wetting. The heterogeneity is associated with a uniform surface of the material, unfortunately all the surfaces have impurities and could influence the surface tension and interact with the liquid influencing the value of water angle contact. The particle's size and shape can affect some properties such as bulk density, permeability, cohesion, attrition, and interaction with liquids. This affects variations over the surface of the material (HEBBAR; ISLOOR; ISMAIL, 2017).

3.3.1 Hydrophobicity and hydrophilic analysis

The wetting characteristics of the material play an important role in a wide of process, such a membrane technology, flotation, enhanced oil recovery, cleaning technology, liquid separation, plans protection etc. in general terms hydrophobicity and hydrophilic terms are associated with water affinity. The materials with good interactions with water are named hydrophilic materials and the materials with poor interactions are name hydrophobic materials; that behavior could be described by water angle contact measure, where the water angle is less than 90° the material is associated with hydrophilic material and with the materials shows an angle high than 90° the value is associated with a hydrophobic material. In membrane process that properties show huge importance, some phenomena are associates with its surface and physicochemical properties exhibiting changes in process of permeability, transport properties, rejection, swelling properties fouling behavior and flux. The determination of the hydrophobic or hydrophilic nature of a membrane is an important parameter in membranes characterization.

3.4 VISCOSITY OF A POLYMER IN SOLUTION

Before to describe the viscosity of a polymer in solution will take a brief approach to describe the principles of polymer solution. The process of solubility in polymers consist in two steps as shown in Figure 9 first one the solvent penetrates the surface of the polymer and start to occupied spaces between the polymer chains, the polymer star to increase its volume and form a swelling gel, increases the

quantity of solvent, the solvent star penetrates between the polymeric chain reducing the intermolecular forcer between the polymeric chain, the polymeric chain increases its liberty between each and another helping to increase its volume. The volume will increase up to its limit and then the swelling gel will disintegrate forming a True solution (CANEVAROLO, 2019).

Figure 9: Flux diagram for a true polymeric solution, showing all the steps for get a polymeric true solution.
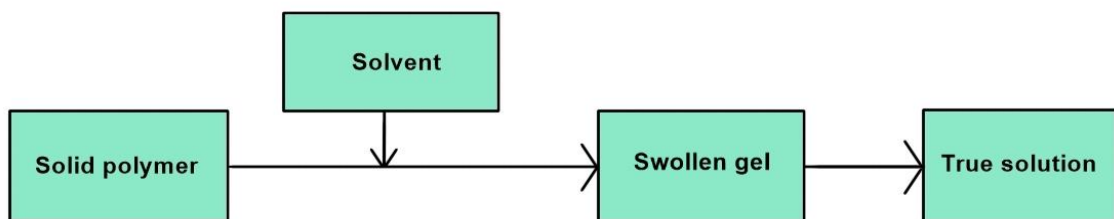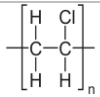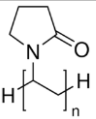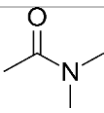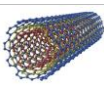
Source: Done by the author.

4 MATERIALS AND METHODS

PVC (Poly(vinyl chloride)) with Mw 80,000 Da (purchased from *Sigma-Aldrich, USA*), PVP (Poly(vinylpyrrolidone)) Mn 40,000 Da (*purchased from Dinâmica Química Contemporânea, Brazil*), both used to form the polymeric blend and Dimetilacetamida-N,N 99% (purchased from *Neon reagents analíticos*, Brazil) such as solvent, Multi-Walled Carbon Nanotubes (MWCNTs) (*purchased from US Research Nanomaterials, Inc,* USA), toluene and cellulose commercial filter. Table 3 Shows the materials used for the formation of the composite.

Table 3: Materials used in the formation of the composite in this study.

Name	Structure	Function
Poly(vinyl chloride)		Precursor
Poly(vinylpyrrolidone)		Precursor
Dimethylacetamide-N,N		Solvent
Toluene		Used to create emulsion/ disperse MWCNTS
MWCNTs		Reinforced phase
Cellulose filter	--	Substrate

Source: Done by the author.

4.1 COMPOSITE PREPARATION

The preparation of the composite involved an experimental design to optimize the performance of the fibers, parameters such as fibers diameter and quantity of beads were taken into consideration as the output in the experimental design. The solution was prepared with a weight relationship DMAC/PVC plus a 3%,

5% and 7% of PVP as a percentage of the total weight. The solutions were kept in magnetic stirring for 4 hours in 75°C, then 10 mL of solution was collected in a syringe to be used in electrospinning apparatus; 15 kV-25 kV, 1.7 mL/h and 25 cm was the voltage used in the A/C electrical source, the feed rate of the polymer solution and the distance between the tip of the needle to the collector, respectively. The electrospun fiber was collected in a commercial cellulose filter for easy removal, 4 hours was the collection time. Figure 10 shows the process of solubilization of the polymer.

Figure 10: Schematic representation of the process of polymer solubilization
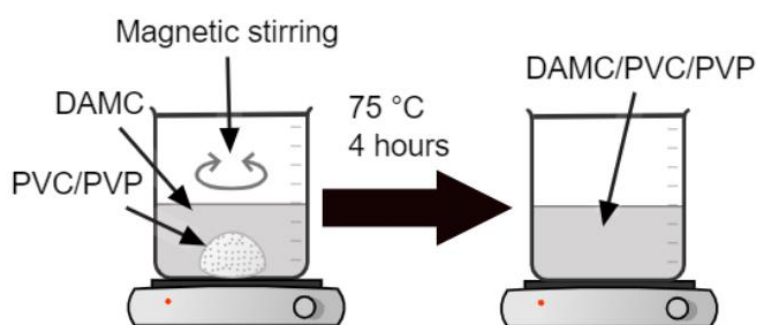
Source: Done by the author.

Caption: Schematic representation of the process of polymer solubilization, in the left site the process of magnetic stirring and heat (75°C) assists the process of solubilization in the system PVC/PVP and DMAC. In the right site schematic representation polymer in solution.

Two methodologies were considered to disperse the MWCNTS in a liquid, the first one involved taking 0.9 mg of MWCNTS and adding in 30 mL of toluene in a bottom flask. It was kept for 3 hours in an ultrasonic bath to disperse the nanomaterial. The second methodology involved addition of 0.9 mg of MWCNTS in 200 mL of DI water in a bottom flask and kept 3 hours in ultrasonic bath. Figure 11 shows a schematic representation of a multi-walled carbon nanotubes dispersion process for toluene.

Spray, self-assembled and casting were the methods considered to deposit MWCNTS on the fiber's surface. In this case the first methodology of dispersion was conducted for all the deposition methods; For casting deposition 10 mL of solution toluene/WMCNTS was deposited over the surface of the fibers. For spray, the fibers

were received 10 mL of MWCNTs with the solution toluene/MWCNTS, Figure 12 shows the schematic representation of the deposition process in spray. Self-assembled deposition consists in a liquid-liquid interface system (toluene/ water) (CAVA et al., 2012), The MWCNTS (0.30 mg) was dispersed in toluene (15 mL) in a 50 mL round bottom flask containing 15 mL of deionized water The two liquid was kept in an ultrasonic bath for 90 min, after the process of emulsion process happens the system was undisturbed and transferred from a round bottom flask to a beaker of 200 mL up to the formation of the 2 phases, then a film of MWCNTs is formed in the interphase; then an electrospun membrane is soaked in the liquid-liquid system and the MWCNTS are recovery over the surface of the membrane.

Figure 11: Schematic description of a flux diagram showing the process for disperse MWCNTs on toluene.
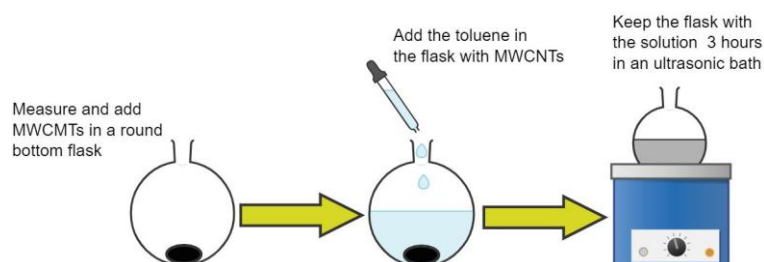
Source: Done by the author.

Caption: Schematic description of a flux diagram showing the process for disperse MWCNTs on toluene. In the first step the addition of MWCNTs in a bottom flask in the second step toluene is added in the bottom flask, and in the third step the bottom flask is kept in ultrasonic bath for 3 hours.

Figure 12: Schematic representation of MWCNTS deposition over a PVC/PVP electrospun membrane.
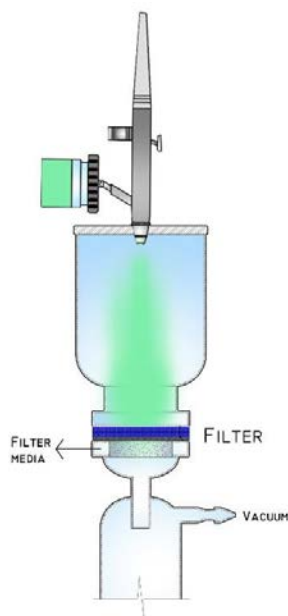
Source: Done by the author.

For the second methodology of dispersion, it was considered to deposit the solution with casting method, it was considered 5 mL and 4 concentrations for analyze the dispersion of MWCNTS over the surface of the fiber (100%, 80%, 50% and 30%). The deposition method was assisted with a vacuum filter such as spray method to warrant the dispersion over the full matrix of PVC/PVP.

All the samples were dry in air for 48 hours, all the samples were analyzed with SEM to analyze the dispersion for MWCNTS on the membrane PVC/PVP.

Figure 13 shows a flux diagram where are shown the principles steps in the formation of the PVC/PVP electrospun fibers and the deposition of the MWCNTS over the matrix.

Figure 13: Flux diagram of synthesis and characterization of a nano-composite membrane in this project.
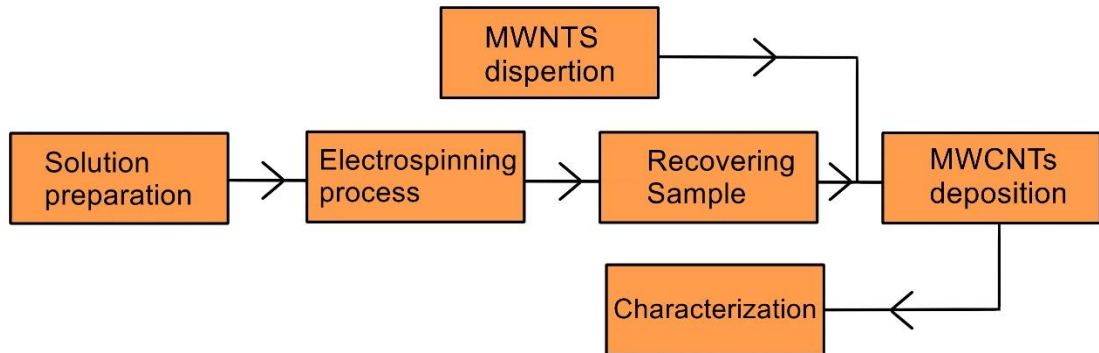
Source: Done by the author.

4.2 COMPOSITE CHARACTERIZATION

Firstly, the structure and morphology of the fibers was analyzed with an optic microscopy for all the samples, all the samples were recovery to determine the best options from the experimental design, where the bests options analyzed in optic microscopes were chosen for be analyzed over SEM, parameter such as beads and diameters of the fibers were analyzed. Another parameter analyzed with SEM was the dispersion of the MWCNTs over the surface of the fibers. The hydrophobic nature is an extremely important parameter in membrane process and adsorption process; that parameter was analyzed with water contact angle; each sample was tested 5 times to has a margin in the results.

The chemical structure of the fibers was analyzed with Fourier-transform infrared (FTIR) spectroscopy in attenuated total reflectance (ATR). The range was from 400 to 4000 cm^{-1}. That spectrum gives us important information about the presence of some characteristic functional groups present in the polymers and also shows some interactions with the polymer blend. Samples with, PVC, PVP, PVC/PVP, and PVC/PVP/MWCNTs were analyzed in contrast to determine the differences in the spectrum.

The viscosity of the polymer solution is a parameter that plays an important role in the formation of the fibers with less defects and uniform morphology; the rheological behavior of the solution was measure with the next parameter, shear rate from 0 to 1000 s^{-1} at 25°C. The shear stress (τ) shares rate (γ). The data were collected and fitted with the power of law model, as is shown in Equation 3.

$$\tau = k(\gamma)^n$$

(3)

Where τ is the share stress (Pa), is the share rate (s^{-1}), k is the consistency.

Thermal gravimetric analysis (TGA) was used to determine the thermal stability of the fibers in an inert atmosphere, parameter: from room temperature to 750°C, 20 mL/min and an average of 3 mg of samples were analyzed for 4 samples two for each analysis (PVC/PVP and PVC/PVP/MWCNTS). Differential Scan Calorimetry (DSC) was used to determine its characteristics temperatures of the fibers, flow rate 20 mL/min of nitrogen, and temperatures from 25°C to 180°C was the parameters consider in the experiment.

4.3 ADSORPTION TEST

A simple process adsorption was performed with of vegetal oil (100 µL), and 35 mg of electrospun PVC/PVP, a beaker of 50 mL was filled with deionized water and 100 µL of vegetal oil was added in the beaker. At this experiment 36 mg of electrospun fibers were used to absorb the oil in the beaker. It processes shows the potential use of electrospun technology to develop membranes with good affinity with hydrophobic liquids. Figure 14 shows the schematic representation of the adsorption test.

Figure 14: Schematic representation of the qualitative adsorption test.
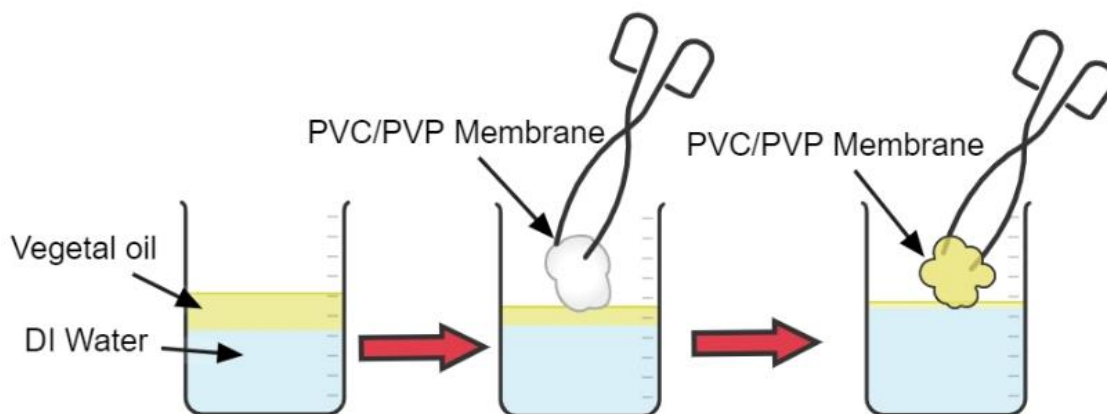
Source: Done by the author.

Caption: Schematic representation of the qualitative adsorption test, a beaker was filled partially with deionized water, after that, a volume of vegetal oil was added and the separation of the phases was evidenced, a mass of 36 mg of electrospun PVC/PVP was soaked in the vegetal oil, and some of the vegetal oil was adsorbed by the electrospun membrane PVC/PVP.

4.3.1 Adsorption of Vegetal oil

A beaker of 50 mL was filled with a vegetal oil, the beaker was kept in a scale, before that a piece of electrospun membrane was weighted in the scale. That piece of electrospun membrane was soaked in the vegetal oil and keep for 15 seconds then a percentage of vegetal oil was adsorbed by the electrospun membrane. that process was repeated 6 time with a virgin membrane and similar weights. It was tested electrospun membrane PVC/PVP, and electrospun membranes with MWCNTs deposition according with the second methodology of dispersion and casting vacuum assisted deposition method. Membrane tested: PVC/PVP, PVC/PVP+3 mL, PVC/PVP+5 mL, PVC/PVP+10 mL, PVC/PVP+15 mL, PVC/PVP+20 mL of MWCNTs dispersion in water. It was calculated how many times the membrane adsorbed its own weight. The values of MWCNTs are shown in the Results part.

5 RESULTS AND DISCUSSION

5.1 EXPERIMENTAL DESIGN AND MORPHOLOGY

The experimental design was developed to obtain the better performance in the formation of fiber with less diameter and less morphological defects, the literature was consulted to determine the starting points (ALARIFI et al., 2018; QUOC PHAM et al., 2021). The concentration DMAC/PVC, the percentage of the total weight of PVP and, voltage was the variables consider in the experimental design. The aim of the experimental design considered to produces fiber with a small diameter and low quantity of beads. Table 4 shows the total number of experiments takes into consideration and the total of levels takes into consideration for all the variables. For a concentration DMAC/PVC and the percentage of the PVP was considered 3 levels and for the voltage were consider 2 levels. All the experiments was repeated 2 times.

Table 4: The experimental design parameters, the experimental design considered 3 parameter: concentration DMAC/PVC with 3 levels.

Experiment	A	B	C	DMAC/PVC	PVP %Wt	Voltage	Code
1	-1	-1	-1	75/25	3	15	75/25PVC3PVP15
2	0	-1	-1	80/20	3	15	80/20PVC3PVP15
3	1	-1	-1	85/15	3	15	85/15PVC3PVP15
4	-1	0	-1	75/25	5	15	75/25PVC5PVP15
5	0	0	-1	80/20	5	15	80/20PVC5PVP15
6	1	0	-1	85/15	5	15	85/15PVC5PVP15
7	-1	1	-1	75/25	7	15	75/25PVC7PVP15
8	0	1	-1	80/20	7	15	80/20PVC7PVP15
9	1	1	-1	85/15	7	15	85/15PVC7PVP15
10	-1	-1	1	75/25	3	25	75/25PVC3PVP25

11	0	-1	1	80/20	3	25	80/20PVC3PVP25
12	1	-1	1	85/15	3	25	85/15PVC3PVP25
13	-1	0	1	75/25	5	25	75/25PVC5PVP25
14	0	0	1	80/20	5	25	80/20PVC5PVP25
15	1	0	1	85/15	5	25	85/15PVC5PVP25
16	-1	1	1	75/25	7	25	75/25PVC7PVP25
17	0	1	1	80/20	7	25	80/20PVC7PVP25
18	1	1	1	85/15	7	25	85/15PVC7PVP25

Source: Done by the author.

Caption: The experimental design parameters, the experimental design considered 3 parameters: concentration DMAC/PVC with 3 levels (75/25, 80/20, and 85/15), the concentration of PVP considered such as a percentage of the total weight (3%Wt, 5%Wt, and 7%Wt) and the voltage with 2 levels (15 kV and 25 kV), the code for all the experiments considers de concentration DMAC/PVC the percentage of the total weight of PVP and the voltage used.

After the conduction of all the experiments, the samples were analyzed over an optic microscope. It was remarkable that the concentration 75/25 (DMAC/PVC) did not conform fiber, probably the concentration of polymer was extremely high, and the solvent evaporates in the tip of the needle before to travel and, a high quantity of dry material was accumulated in the tip of the needle. The configuration 85/15 (DMAC/PVC) shows high quantities of beads, probably that phenomenon could be associated with a bad interaction with the rheological properties of the polymer solution and the electrical field, causing interference in the formation of the Taylor cone forming high quantities of beads. The configuration 80/20 (DMAC/PVC) shows the better structural performance, the quantities of beads was less and was possible to analyze some samples without beads. That analysis confirms that the concentration of solvent/polymer plays a determinant role in the formation of fibers with high quality.

Figure 15 shows an optic microscope image where is possible to analyze the difference of the morphology of 3 different samples. it is possible to analyze in Figure 15 (A) fibers without beads, in Figure 15 (B) fiber with a high concentration of

beads, and in Figure 15 (c) is possible to analyze some beads. Figure 15 (A), configuration 80/20 shows fiber with good shape and morphology, after that analysis the best samples were selected to be analyzed over SEM, parameter such as diameter of fibers and beads presence was analyzed over SEM.

Figure 15: Optic microscope photographs where is possible analyze different electrospun samples, 80/20/PVC3PVP15, 85/115PVC7PVP15 and, 80/20PVC7PVP15.
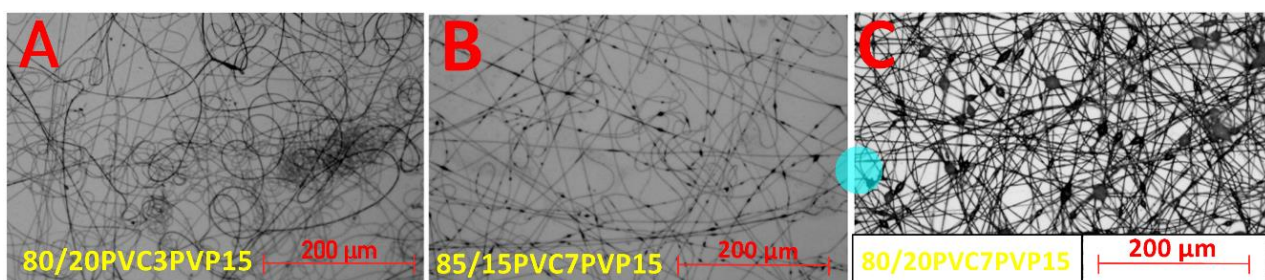
Source: Done by the author.

Caption: Image (A) with configuration 80/20 concentration DMAC/PVC plus 3% of the total weight of PVP and 15 kV shows low quantity of beads and good morphology, image (B) with configuration 85/15 concentration DMAC/PVC plus 7% of the total weight of PVP and 15 kV shows high quantity of beads and small diameters; meanwhile image (C) with configuration 80/20 concentration DMAC/PVC plus 7% of the total weight of PVP and 15 kV shows high quantity of beads and big diameters

Figure 16 shows SEM image of the fibers 80/20 configurations, it is possible to analyze a relationship between the diameter of the fibers and the percentage of PVP. The diameter of the fibers was analyzed using the software ImageJ and was chosen 200 fibers for to get average diameter; The SEM images shows the influence of the variables (voltage and percentage of the total weight of PVP) over the quality of the fiber, the morphology is associated with that parameter. (A) 80/20PVC3PVP25, (B) 80/20PVC5PVP25, (C) 80/20PVC7PVP25, (D) 80/20PVC3PVP15, (E) 80/20PVC5PVP15 and (F) 80/20PVC7PVP15 are the experiments associated with the configurations 80/20 DMAC/PVC. It is possible to analyze that exist a relationship between the applied voltage and fiber diameter, in this case Figure 16 (D, E, F) shows that fibers with 15 kV shows less morphological defects.

Figure 16: SEM images of 80/20 DMAC/PVC concentration, 3, 5, and 7 percentage of the total weight of PVP for each voltage (15-25 kV).
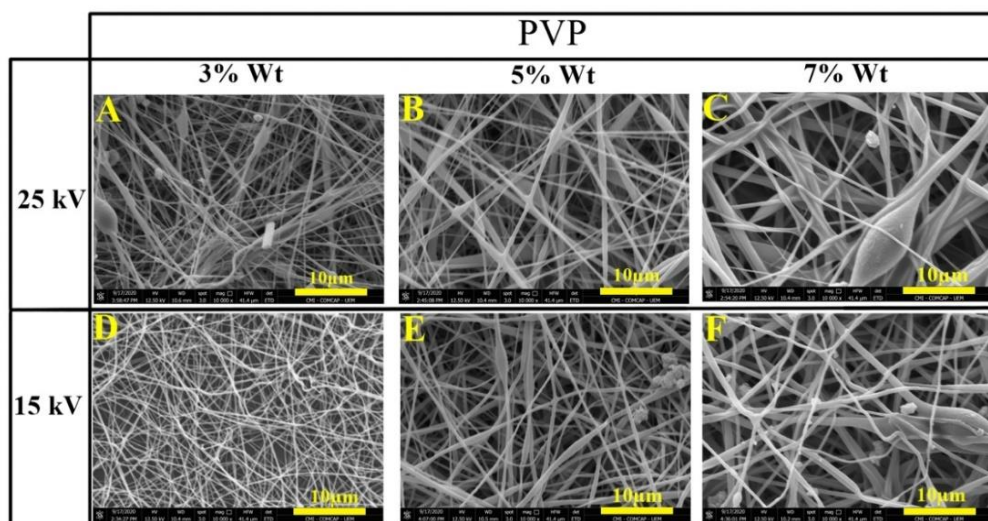
Source: Done by the author.

Caption: Image (A) shows electrospun fibers with small fibers diameter the presence of beads is evidenced, (B) the diameter of the fibers is bigger than Image (A) and the presence of beads is less evident, (C) Figure C shows fibers with big diameters and the presence of beads is evident. Image (D) shows good morphology small fibers diameters, and the presence of beads are not evidenced. (E) the presence of beads is evident, and the diameters of the fibers are bigger than the image (D), image (F) shows fibers with small and big diameters the presence of beads is also evidenced.

Figure 17 shows the diameter distribution for the samples with 15 kV, and the average diameter of the fibers. Figure 17 confirms that exist relation between the diameter size and the percentage of PVP. Figure 17 (A) shows a SEM image and diameter distribution for the sample 80/20PVC3PVP15, Figure 17 (B) shows a SEM image and diameter distribution for the samples 80/20PVCPVP15, Figure 17 (C) shows a SEM image and diameter distribution for the sample 80/20PVC7PVP15. As is increased the percentage of PVP increase the diameter of the fiber.

Figure 17: SEM image of 80/20 concentrations and diameters distribution.
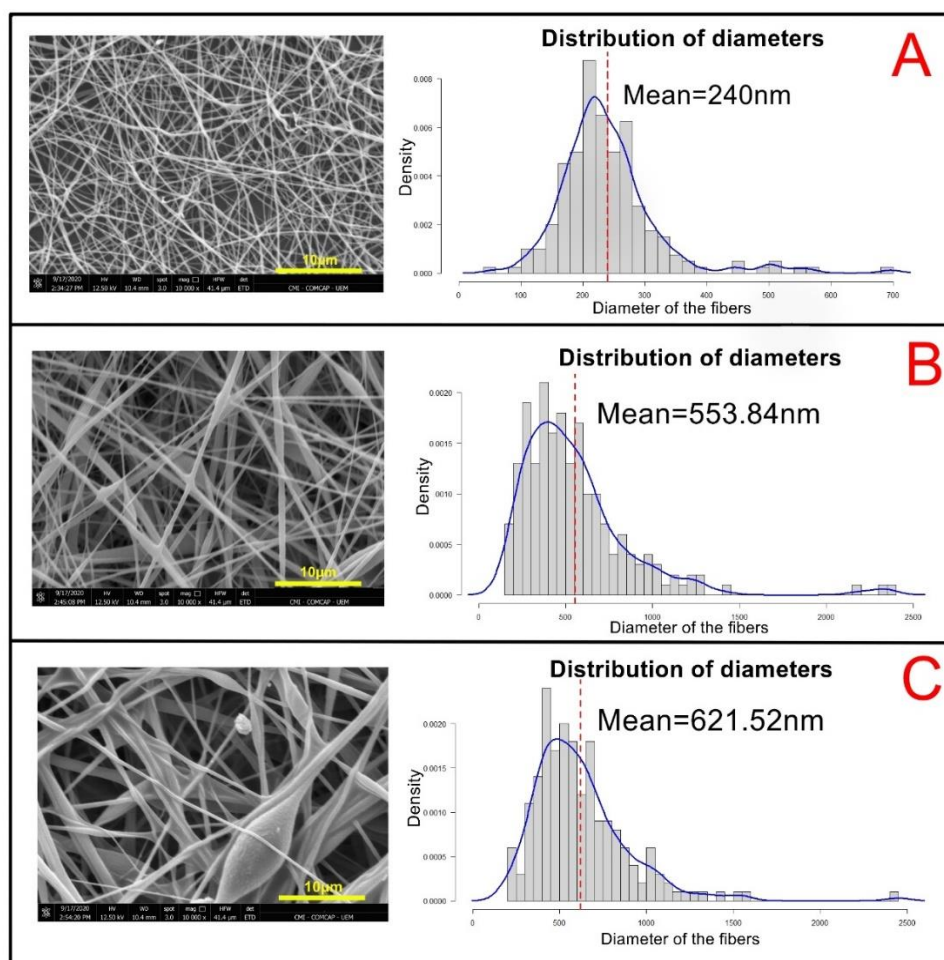
Source: Done by the author.

Caption: Image (A) shows a SEM image of the electrospun fibers with configuration 80/20PVC3PVP15 also is show a diameters size distribution and the mean diameter of 240 nm. Image (B) shows a SEM image of the electrospun fibers with configuration 80/20PVC5PVP15 also is show a diameters size distribution and the mean diameter of 553.84 nm. Image (C) shows a SEM image of the electrospun fibers with configuration 80/20PVC7PVP15 also is show a diameters size distribution and the mean diameter of 621.52 nm. It was evident that the diameter has a relation with the percentage of PVP such as increase the percentage of PVP increase the values of the diameter.

It was evidenced in the Figure 17 (A) the electrospun fiber with the configuration 80/20PVC3PVP15 shows less diameter and morphological defects that why was chosen for deposit MWCNTs. Scanning electron microscopy also was used to explore the deposition of MWCNTS over the electrospun fibers. Figure 18 shows a contrast with the three deposition methods, all this deposition methods was conducted with a MWCNTS dispersed in toluene such as was describe in 4.1 first dispersion methodology , (A) Spray, the dispersion over the fibers looks more uniform and has less conglomeration of MWCNTS, In figure 18 (B) casting, it is possible to analyze a high concentration of MWCNTS over the fibers, probably that behavior is

associated with a dispersion of MWCNTS in the toluene, Figure 18 (C) show the dispersion of MWCNTS under the dispersion technique self-assembled, as is possible to analyze that exist a high concentration of MWCNTS over the fibers forming lumps. It was evident that all the dispersion in toluene shown a poor dispersion of MWCNTS probably the concentration was very high difficulty the dispersion in low volume of toluene.

Figure 18: SEM images of 80/20PVC3PVP15 configuration and dispersion of MWCNTs by different methods.
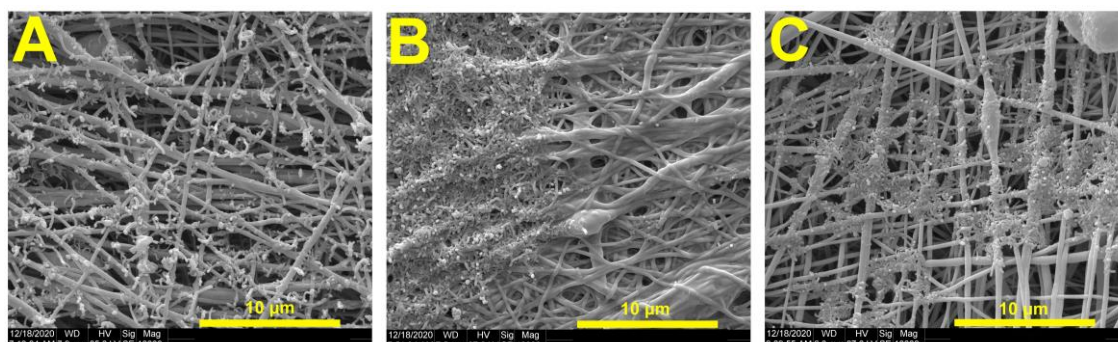
Source: Done by the author.

Caption: Image (A) shows electrospun fiber 80/20PVC3PVP15 with MWCNTs dispersion deposited by spray. Image (B) shows 80/20PVC3PVP15 electrospun fibers with MWCNTs dispersion deposited by casting method. Image (C) shows 80/20PVC3PVP15 electrospun fibers with MWCNTs dispersion deposited by self-assembled method.

Figure 19 shows an example of the membrane performed by electrospinning and the dispersion of MWCNTs was performed by spray.

Figure 19: PVC/PVP/MWCNTS membrane in the left site and SEM image where is showing the MWCNTs dispersion deposited by spray over the electrospun fibers with configuration 80/20PVC3PVP15.
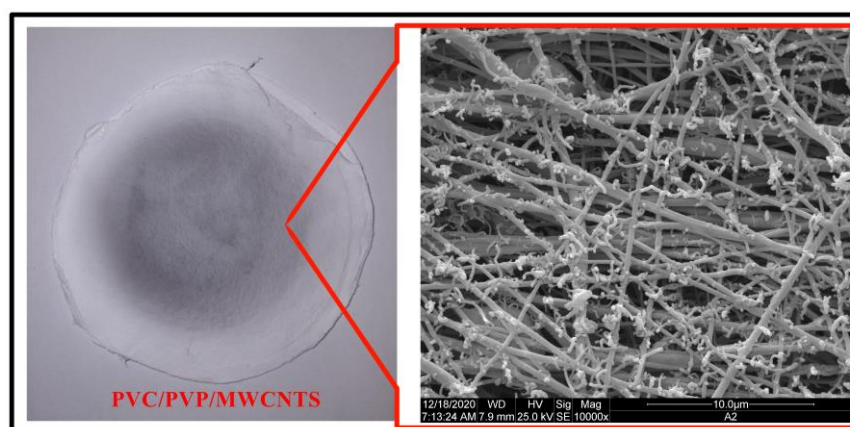
Source: Done by the author.

The second methodology of dispersion in DI water was deposit with casting method assisted with vacuum filter, over the PVC/PVP membrane and was analyzed over SEM. Figure 20 shows the dispersion of MWCNTS for different concentration over the surface of PVC/PVP fibers, A (100%), B (80%), C (50%) and D (30%). Each sample was analyzed 2 times to confirm the results.

Figure 20: Dispersion of MWCNTs for different concentrations on electrospun fiber with configuration 80/20PVC3PVP15.
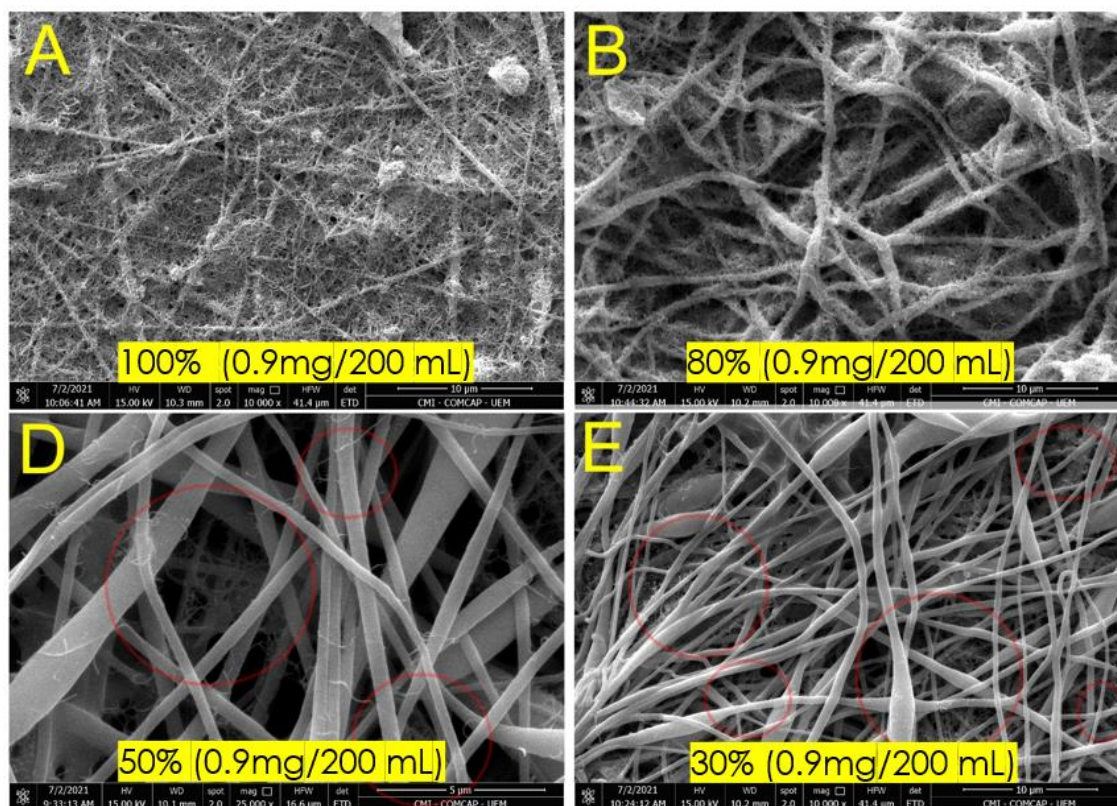
Source: Done by the author.

Caption: Image (A) Shows electrospun fibers completely covered of MWCNTs with a concentration of 0.9 mg/200mL. Image (B) shows electrospun fibers partially cover by MWCNTs with 80% of the mother concentration (0.9 mg/200mL). Image (D) shows electrospun fibers with a little presence of MWCNTs with 50% of the mother concentration (0.9 mg/200mL). Image (E) shows electrospun fibers with a very little presence of MWCNTs with 30% of the mother concentration (0.9 mg/200mL).

Such as is possible to compare in Figure 20 (A) the concentration of MWCNTS was extremely high and is possible to analyze that the full fibers were cover by MWCNTS, and probably that condition could play an important role in flux performance. Figure 20 (B) exhibits an interesting condition where the fiber was partially cover by MWCNTS, it is possible to analyze a furry surface of the nanofibers.

Figure 20 (C, D) shows fiber with less quantity of MWCNTS, the red circles show some areas where are found MWCNTS.

5.2 PHYSICOCHEMICAL CHARACTERIZATION

5.2.1 ATR-FTIR spectroscopy

ATR-FTIR spectroscopy was used to determine the chemical composition of the composite and detect the polymers present in the blend, in this case is interesting to expose the contrast with all the materials used for the conformation of the fibers and is possible to explore those specifics groups present in the materials that can absorbs vibrational energy, Figure 21 Shows the ATR-FTIR spectrum for PVC, PVC/PVP, PVC/PVP/MWCNTs and PVP and, also is shown the regions for the specific functional groups present in the polymers and polymeric blends. The composite PVC/PVP shows the characteristic bands in 610 cm^{-1} that is associated with a bound C-Cl rocking vibrational mode, that group belongs to PVC, between 1700-1610 cm^{-1} exist a group C=O stretching vibrational mode associated with the chemical structure of the PVP, between 2800 and 3000 cm^{-1} exist a group C-H stretching vibrational mode associated in both polymers PVC and PVP, and between 3300 and 3600 cm^{-1} exist a group O-H stretching vibrational mode associated with the chemical structure of PVP. That shows that the blends conformed by PVC/PVP has the specific functional groups of PVC and PVP. The C=O (Carbonyl group) is observed between 1700-1610 cm^{-1} and in the polymer, blend is observed to shift to high frequency, that behavior suggest a significant intermolecular/intramolecular interaction bending. For this case the miscibility of the blend PVC/PVP is possible by the presence of dipole-dipole interactions between the C-Cl of PVC and C=O of PVP (BHAVSAR; TRIPATHI, 2018). Similar results have been reported in the literature (ALARIFI et al., 2018; NAJAFI; ABDOLLAHI, 2020a; WYPYCH, 2016a; ZHANG et al., 2020a). That analysis was taken in consideration to detect the chemical composition in the polymer blend.

Figure 21: ATR-FTIR spectrum for PVC, PVC/PVP, PVC/PVP/MWCNTS and PVP.
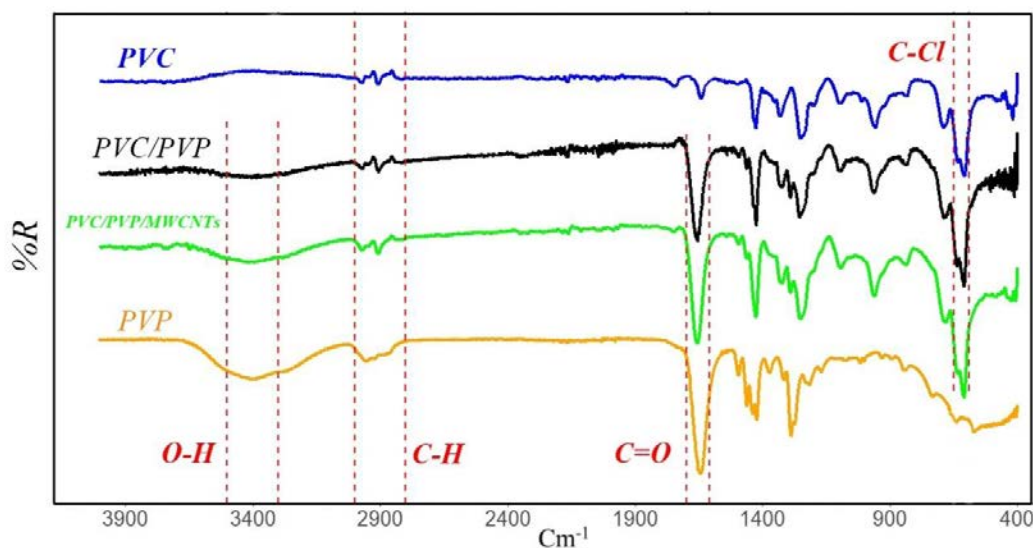
Source: Done by the author.

Caption: the figure shows the spectrum of each polymer and the blend PVC/PVP also it is possible analyze the composite PVC/PVP/MWCNTs, all the polymers shows its specifics and characteristic areas where absorb energy, in the blend PVC/PVP it is possible analyze a shift that is associated with intermolecular interaction dipole-dipole.

5.2.2 Water angle contact

The water angle contact was measure five times for each sample, it was evidenced that all samples show a hydrophobic behavior, probably the external surface of the fibers are conformed by PVC that governs a hydrophobic behavior and, the internal core of the fibers are conformed by PVP. Figure 22 shows the bar chart of water contact angle for all the experiments that conformed fibers, as is possible to analyze in the Figure 22 all the experiments have an hydrophobic behavior; similar behavior have been report by (ALARIFI et al., 2018). Figure 22 also shows an example of a digital image of a regular behavior of a sample of PVC/PVP which shown 120.37° of average diameter. Table 5 shows a resume of all the values and its standard deviation.

Figure 22: Values of water angle contact measure for all the experiments
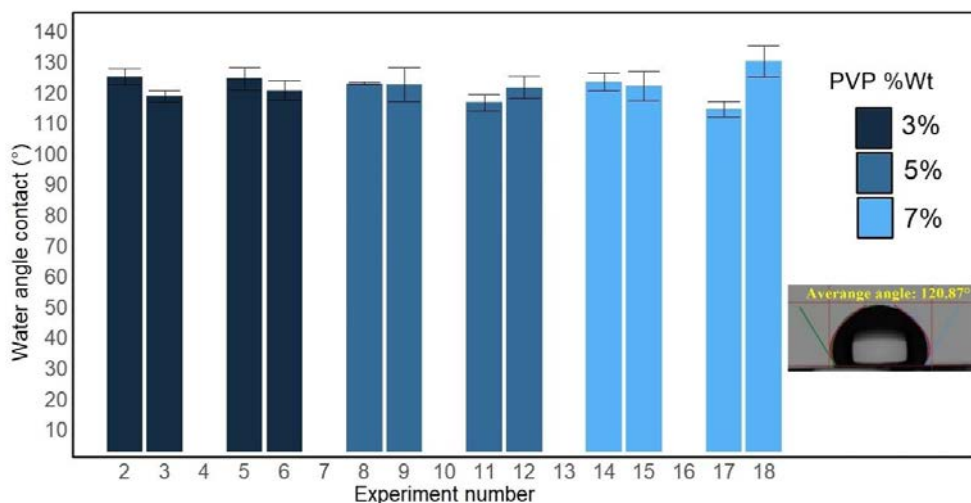
Source: Done by the author.

Caption: the codes of all experiments can be consulted in Table 4. It is evident that all the values show by all the experiments had a hydrophobic behavior, all the values are up to 110°. The figure also shows a digital photo where is possible to analyze a drop of water over a substrate PVC/PVP electrospun fibers with an average water angle contact of 120.87°.

Table 5: Values of water angle contact for all the experiments, the table shows the experimental code for all the experiments the load of PVP, the voltage, and the values of standard deviation for all the experiments.

Experiment code	PVP (%Wt)	Voltage (kV)	Standard deviation	Water angle contact
80/20pvc3pvp15	3	15	2.57	124.92
85/15pvc3pvp15	3	15	1.98	118.38
80/20pvc5pvp15	3	25	3.60	124.21
85/15pvc5pvp15	3	25	3.14	120.30
80/20pvc7pvp15	5	15	0.38	122.63
85/15pvc7pvp15	5	15	5.56	122.39
80/20pvc3pvp25	5	25	2.58	116.39
85/15pvc3pvp25	5	25	3.68	121.40
80/20pvc5pvp25	7	15	2.91	123.11
85/15pvc5pvp25	7	15	4.77	121.86
80/20pvc7pvp25	7	25	2.51	114.14
85/15pvc7pvp25	7	25	4.99	129.80

Source: Done by the author.

5.2.3 Viscosity

The viscosity of a polymer in solution plays an important role in the performance and formation of electrospun fibers, parameter in the solution such as molecular weight and, concentration ratio (solvent/polymer) need to be controlled to get fibers with less defects and less diameter (RAHMATI et al., 2021; TIWARI; VENKATRAMAN, 2012). The Figure 23 shows the curve shear stress versus shear flow (A) and the flow curve (B); as is possible in Figure 23 (B) the solution obeys a pseudoplastic behavior as is increased the share rate decrease the share stress (KING, 2002), and the experimental data fits with the model of power of law (KING, 2002); Table 6 shows the rheological coefficients associates with the power of law model. the solution used to determine the viscosity of fibers is associated with the experiment coded 80/20pvc3pvp15 that was the solution with better performance in the formation of fibers.

Figure 23: Experimental for determine the rheological properties of the blend PVC/PVP.
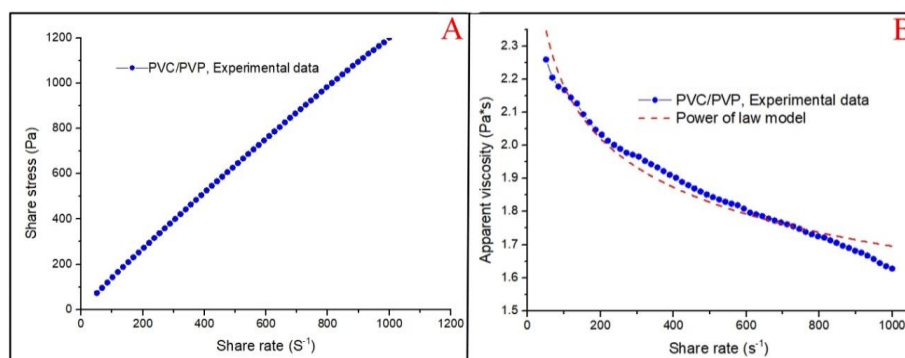
Source: Done by the author.

Caption: (A) where is shown a pseudoplastic behavior the slip values down in order the values of the share rate increase, (B) Experimental values where is shown the values of share rate in the X-axis and the apparent viscosity for the Y-axis, the power of law model can describe the behavior and is show in the red dashed line.

Table 6: Values of the constants associated with the power of law model for the solution coded 80/20/PVC3/PVP15, k= consistency index and n = flow behavior index.

Experiment code	K (Pa*s^n)	n
80/20pvc3pvp15	3.867±0.072	0.883±0.003

Values are given as the mean ± SD from triplicate determinations.
Square of coefficient correlation: 0.964
k: consistency index; n: flow behavior index.

Source: Done by the author.

5.2.4 Thermal analysis, thermogravimetric (TGA, DTGA)

TGA and DTGA thermograms of PVC/PVP and PVC/PVP/MWCNTS are shown in Figure 24 (A) and Figure 24 (B) respectably. Figure 24 (A) shows the TGA thermograms; It is possible to compare the behavior of both membranes, PVC/PVP/MWCNTS exhibited high thermal stability in the first loss of mass, probably the incorporation of MWCNTS enhance the thermal stability in the phenomenon named dehydrochlorination near to 250°C (NAJAFI; ABDOLLAHI, 2020b; QUOC PHAM et al., 2021), that behavior is better understood in Figure 24 (B), where is shown the values associated with the mass change as a function of temperature, for PVC/PVP the values are higher and start before PVC/PVP/MWCNTS membrane. For PVC/PVP was analyzed tree steps of decomposition; from 190 °C to near 450°C was observed the first loss of mass that lose could be associated with the phenomenon of dehydrochlorination; from   450 °C to 525°C was analyzed the second loss of mass for the membrane composed by PVC/PVP, and a third loss of weight from 525 °C to near to 650. For the membrane composed by PVC/PVP/MWCTNS was analyzed high thermal stability in the first stage of loss of weight, the membrane starts the first loss of mass near to 190°C and it is prolonged up to reach near to 350°C, the second stage of mass loss starts near to 350°C and is prolonged up to reach near to 560°C. that membrane just exhibited two stages of decomposition. Table 7 shows the most important TGA analysis data. Exist a better thermal stability for a PVC/PVP/MWCNTS in the first 50% of loss of weight.

Figure 24: The thermogram TGA for the PVC/PVP (red line) and the composite PVC/PVP/MWCNTs (blue line) electrospun fibers,.
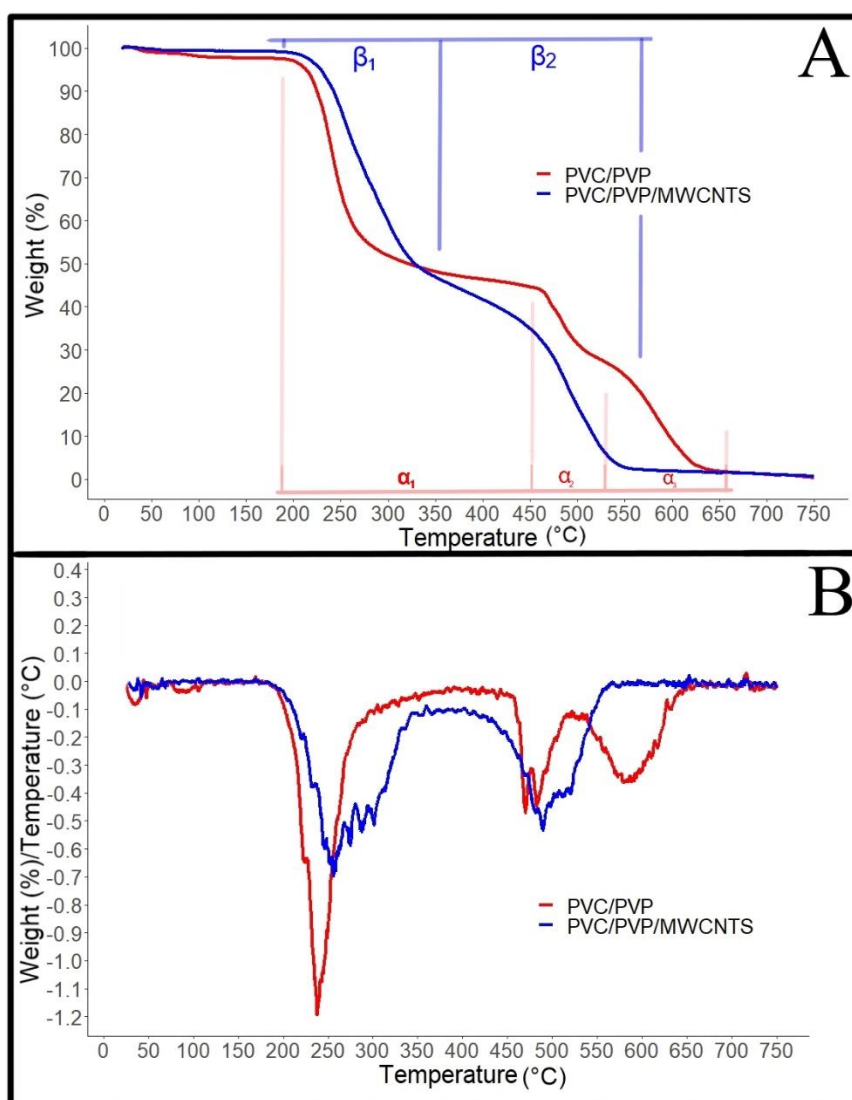
Source: Done by the author.

Caption: PVC/PVP (red line) and the composite PVC/PVP/MWCNTs (blue line) electrospun fibers, the electrospun fibers PVC/PVP shows 3 stages of decomposition the first one (α_1) takes place from 190°C to 450°C phenomenon associated with dehydrochlorination the second stage (α_2) of degradation takes please from 450°C to 525°C and the third stage (α_3) of decomposition takes please from 525°C to 650°C; in comparation the electrospun fibers PVC/PVP/MWCNTs shows better thermal stability in the first stage (β_1) of degradation starting from 190°C to 350°C the slip is less pronounced for the PVC/PVP/MWCNTs electrospun fibers, the second stage (β_2) of degradation takes place from 350°C to 560°C and the third stage of degradation was not evident. and DTGA thermogram, image (B) shows the blend PVC/PVP electrospun fibers (red line) with the three stages of degradation also it is possible to compare the values of the slip with the blend PVC/PVP/MWCNTs electrospun fibers, where the values of the blend PVC/PVP are high in the first stage of decomposition showing that the loss of mass is faster that the PVC/PVP/MWCNTs electrospun fibers. for the blend PVC/PVP/MWCNTs just two stages of decomposition are evidenced.

Table 7: Shows the principles values of TGA and DTGA for blend conformed by PVC/PVP and PVC/PVP/MWCNTs.

Material	T 5%	T 10%	T 50%	T Min	Char yield (%)
PVC/PVP	213.30	224.59	321.54	237.96	0.39
PVC/PVP/MWCNTS	228.90	242.57	328.43	256.23	0.69

Source: Done by the author.

Caption: Shows the principles values of TGA and DTGA for blend conformed by PVC/PVP and PVC/PVP/MWCNTs. The table shows the values for the temperatures associates with the 5%, 10%, 50% of mass loss and is show the minimum values for the DTGA, it is possible to analyze the percentage of the char yield for each blend.

5.2.5 Thermal analysis, Differential Scanning Calorimetry (DSC)

Figure 25 shows a thermogram of a DSC for samples conformed by PVC/PVP and PVC/PVP/MWCNTS it is possible to analyze two interesting points in each sample, both points are associated with exothermic events, that two points could be associated with the glass transition temperature of each polymer, for the sample conformed by PVC/PVP it is possible the first transition temperature near to 83°C temperature associated the glass transition temperature of PVC (CARRIZALES et al., 2008), the second point could be associated with the glass transition of PVP 94°C (OSUNTOKUN; AJIBADE, 2016). The same behavior is obeying by the samples conformed by PVC/PVP/MWCNTS but in this case the peaks are less evident, and the values are less than PVC/PVP, they are closer each and other, that behavior is found if are contrasted different concentrations of polymeric blend (AOUACHRIA; BELHANECHE-BENSEMRA, 2006), but in this case probably the good thermal conductivity of MWCNTS shows a better interaction polymer/polymer showing less intensive peaks.

Figure 25: The thermogram DSC for the PVC/PVP (red line) and the composite PVC/PVP/MWCNTs (black line) electrospun fibers,.
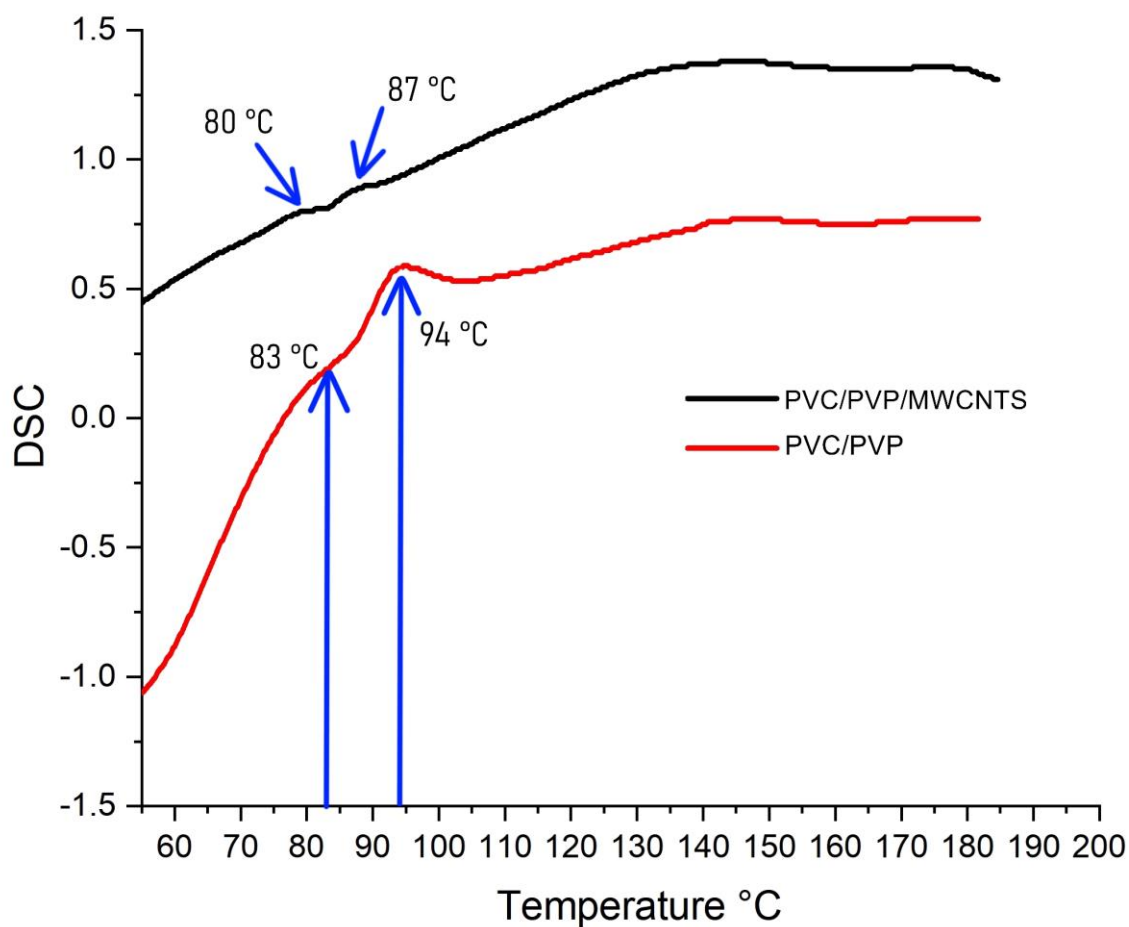
Source: Done by the author.

Caption: DSC thermogram of electrospun fibers with configuration 80/20/PVC3/PVP15. PVC/PVP (red line) shows the glass transitions of the PVC in 83 °C and 94 °C for the PVP both peaks are evident. PVC/PVP/MWCNTs (black line) shows low values for the glass transitions of PVC and PVP phenomenon associated with the incorporation of MWCNTs, the values of the peaks are also less evident showing a better polymer interaction.

5.2.6 Adsorption test

The adsorption test was conducted to shows the potential capacity of the PVC/PVP electrospun membrane to reject hydrophobic liquids. Figure 26 shows a beaker with deionized water and vegetal oil (100 µL) in the top and are shown all the process of adsorption of vegetal oil on deionized water. That experiment shows the potential of PVC/PVP membranes to remove oil on water.

Figure 26: The sequence of digital photography showing the adsorption capacity of vegetal of by electrospun fibers with configuration 80/20/PVC3/PVP15.
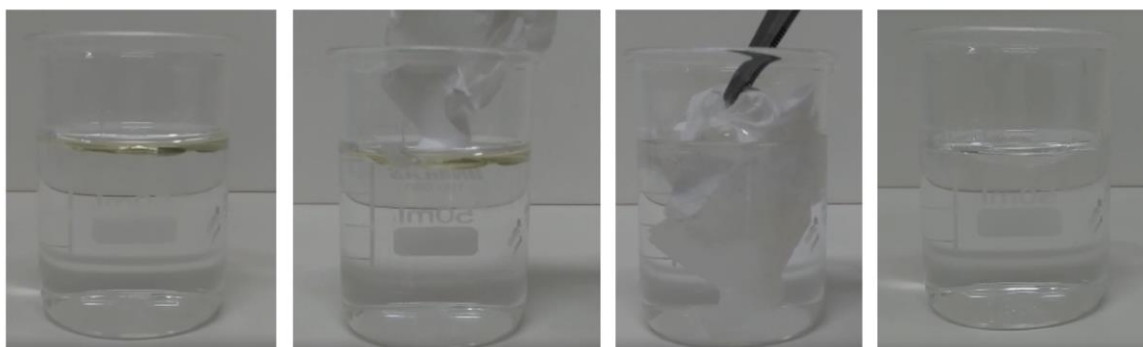
Source: Done by the author.

Caption: It is evident that the electrospun fiber has a strong interaction with a hydrophilic liquid.

5.2.6.1 Adsorption of vegetal oil

Figure 27 shows the performance of the electrospun membranes with and without MWCNTs, the results show that without load of MWCNTs the membrane has interesting adsorption capacity more than 3 times its weight. Meanwhile, it is increased the load of MWCNTs on the membrane the adsorption capacity increases, up to reach values more than 7 times its weight, after that loads of MWCNTs the values start to decrease, the agglomeration of MWCNTs over the matrix limits the spaces where can be occupied by the vegetal oil. While with 0.054 mg of MWCNTs deposited on the matrix was possibly get the highest adsorption capacity 7.14 times of its weight. Table 8 shows all the values for each membrane.

The hydrophobic nature of the MWCNTs plays an important role in the interaction between the matrix and a hydrophobic liquid, the hydrophobic nature of a membrane is improved by the incorporation of MWCNTs (MOFOKENG et al., 2020) and also the high surface of MWCNTs (ANSARI et al., 2011) plays an important role giving more spaces in a matrix for be occupied by the oil molecules. That behavior was evidenced in the process of adsorption of vegetal oil with a PVC/PVP matrix.

Figure 27: The adsorption capacity of different samples of electrospun membranes with configurations 80/20/PVC3/PVP15 with different loads of MWCNTs.
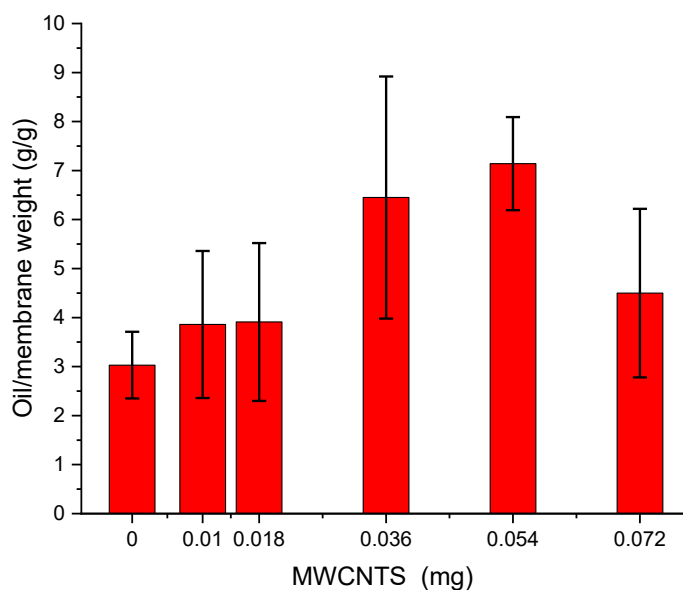
Source: Done by the author.

Caption: Electrospun fibers without a load of MWCNTs show an interesting adsorption capacity of 3.03 times its weight of vegetal oil. Membranes with an MWCNTs charge of 0.01 mg, 0.018 mg, 0.036 mg, and 0.054 mg shows values of 3.86, 3.91, 6.45, and 7.15 of their own weight respectably evidenced that the 0.054 mg charge of MWCNTs was the maximum value reached with this configuration (7.15 times its own weight). It was evidenced that when the charge of MWCNTs increases more than 0.054 the values start to decrease as is shown in the charge 0.072 mg where the adsorption capacity just reaches 4.51 times its weight.

Table 8: The values of MWCNTs weight, the volume added on the electrospun membrane configuration 80/20/PVC3/PVP15.

MWCNTs (mg)	Volume deposited (mL)	Standard deviation	Oil/membrane (g/g)
0	0	0.68	3.03
0.01	3	1.5	3.86
0.018	5	1.61	3.91
0.036	10	2.47	6.45
0.054	15	0.95	7.15
0.072	20	1.72	4.51

Source: Done by the author.

Caption: It was evident that exist optimum condition in relation with the quantity of MWCNTs and the oil weight adsorbed. All the values of oil adsorbed starts to increase in order to increase the quantity of MWCNTs up to reach the maximum value in 7.15 its own weight associated with 0.054 mg of MWCNTs after that quantity of MWCNTs the values start to down.

6 CONCLUSION

Under the experimental design it was possible to obtain fiber with good structural and morphological properties (less quantity of beads and less diameter mean diameter 240 nm), the experimental design shows that the best configuration for synthesized the fibers was associated with next parameter: The mass relationship 80/20 (DMAC/PVC) plus a 3%Wt of PVP, 15kV in the electrical A/C source, the distance from the tip of the needle to the collector was flix in 25 cm and the flux of the syringe was set in 0.02 mL/h for all the experiments. The configuration 85/15 (DMAC/PVC) shows a high quantity of morphological defects, probably the concentration of solvent/polymer do not have a good interaction with the electrical source. It was remarkable that concentration 75/25 did not conform fiber under all condition taken in consideration in the experimental design, probably by the high concentration of polymer the solvent evaporates in the tip of the needle, a high concentration of dry polymer was observed in all the configurations (75/25).

The hydrophobic nature was analyzed for all the experiments that conformed fibers, all the experiment shows a hydrophobic behavior, probably governed by the influence of PVC, probably the surface of the fiber is composed by PVC and the intern part of the fiber are governed by PVP, the low concentration of PVP can govern that behavior. The membrane with configuration 80/20pvc3pvp15 that was the membrane with better structural performance shows a mean of water angle contact of 124.92° that's exhibit a hydrophobic behavior.

The dispersion of MWCNTS were analyzed in two methodologies. The second methodology of dispersion considered disperse MWCNTS in DI water. It was evidenced that with a concentration of 80% shown an electrospun fibers cover partially with MWCNTS, the electrospun fiber shows a furry morphology. The concentration of 100% (0.9mg in 200 mL of DI water) shows fiber full covers by MWCNTS, and the concentration 50% and 30% shown less quantity of MWCNTS. For the First methodology (0.9 mg of MWCNTS and 30 mL of toluene) Spray was the deposition technique that shows the best results in the dispersion of MWCNTS, that technic shows a dispersion with less quantity of flocs and good dispersion over the fiber, casting and self-assembled shown high quantities of flocs over the surface of

the fibers that behavior could be associated with the poor dispersion of MWCNTS in toluene. In contrast the second methodology of dispersion and casting deposition shows betters results, probably the concentration of MWCNTS over DI water was key for a good dispersion.

The thermal analysis, TGA thermograms shows interesting results, the incorporation of MWCNTS over the matrix evidence a better performance in the first step of degradation, where is possible to observe that the values of the slope are less in comparison with the matrix composed by PVC/PVP, it is more evident in the DTGA thermogram. With the incorporation of MWCNTS over the matrix was possible to analyze that also exist a better interaction with the materials that conform the blend; as is possible to analyze in the matrix PVC/PVP exist 3 steps of decomposition, and in the matrix PVC/PVP/MWCNTS was evidenced the presence of 2 steps of decomposition, that behavior could be associated with the good thermal conductivity of MWCNTS that increase the interaction with all the materials. that argument could be extrapolated to the DSC analysis, where the PVC/PVP matrix shows peaks more obvious showing the glass transition temperatures of both materials PVC and PVP while the matrix PVC/PVP/MWCNTS shows peaks less obvious with less values in the glass transition temperatures.

Under the methodology of IR-spectroscopy was possible detect the functional groups present in the membrane composed by 80/20pvc3pvp15 shows the characteristic peak in 610 cm^{-1} that is associated with a bound C-Cl, that group belongs to PVC, between 1700-1610 cm^{-1} exist a group C=O associated with the chemical structure of the PVP, between 2800 and 3000 cm^{-1} exist a group C-H associated in both polymers PVC and PVP, and between 3300 and 3600 cm^{-1} exist a group O-H associated with the chemical structure of PVP.

The rheological analysis for the experiment 80/20pvc3pvp15 shows a pseudoplastic behavior and under the model of power law was possible to characterize the fluid with its coefficients, where k= 3.867±0.072 and n= 0.883±0.003 that parameter is important under the point of view of reproducibility and characterization.

The electrospun PVC / PVP membrane has potential to be used in the removal of hydrophobic liquids from the hydrophilic fluids. The electrospun fiber got removal a huge part of the vegetable oil from deionized. It was discovered that the electrospun membrane PVC/PVP has the capacity of adsorbed three times its weight of vegetal oil while it was added a load of 0.054 mg of MWCNTs dispersion on the matrix was possible to removal up to 7.14 times the weight of the membrane. also was evidenced that when the load of MWCTNs is higher than 0.054 mg the adsorption capacity starts to decrease, behavior associated with less spaces and high agglomeration of MWCNTs on the surface fibers.

7 REFERENCES

ABUNAHEL, B. M. et al. **Effect of Needle Diameter on the Morphological Nanofiber Mats.** International Journal of Chemical and Materials Engineering, v. 12, n. 6, p. 296–299, 2018.

AGRAWAL, G. et al. **Wettability and contact angle of polymeric biomaterials.** In: Characterization of Polymeric Biomaterials. [s.l.] Elsevier, 2017. p. 57–81.

AKOVALI, G. **Plastic materials: polyvinyl chloride (PVC).** In: Toxicity of Building Materials. [s.l.] Elsevier, 2012. p. 23–53.

ALARIFI, I. M. et al. **Water Treatment using Electrospun PVC/PVP Nanofibers as Filter Medium.** International Journal of Material Science and Research, v. 2, n. 1, p. 43–49, 5 ago. 2018.

ANSARI, M. et al. **The defluoridation of drinking water using multi-walled carbon nanotubes.** Journal of Fluorine Chemistry, v. 132, n. 8, p. 516–520, 1 ago. 2011.

AOUACHRIA, K.; BELHANECHE-BENSEMRA, N. **Miscibility of PVC/PMMA blends by vicat softening temperature, viscometry, DSC and FTIR analysis.** Polymer Testing, v. 25, n. 8, p. 1101–1108, 1 dez. 2006.

ARRECHEA, S. et al. **Effect of additions of multiwall carbon nanotubes (MWCNT, MWCNT-COOH and MWCNT-Thiazol) in mechanical compression properties of a cement-based material.** Materialia, v. 11, p. 100739, 1 jun. 2020.

BHAVSAR, V.; TRIPATHI, D. **Structural, optical, and aging studies of biocompatible PVC-PVP blend films.** Journal of Polymer Engineering, v. 38, n. 5, p. 419–426, 2018.

BRAUER, M. et al. **Taking a Stand Against Air Pollution—The Impact on Cardiovascular Disease: A Joint Opinion from the World Heart Federation, American College of Cardiology, American Heart Association, and the European Society of Cardiology.** Journal of the American College of Cardiology, v. 77, n. 13, p. 1684–1688, 6 abr. 2021.

BROOK, R. D. et al. **Particulate matter air pollution and cardiovascular disease: An update to the scientific statement from the american heart association.** Circulation, v. 121, n. 21, p. 2331–2378, 1 jun. 2010.

CANEVAROLO, S. V. **Polymers in Solution.** In: Polymer Science. München: Carl Hanser Verlag GmbH & Co. KG, 2019. v. 43p. 55–88.

CARRIZALES, C. et al. **Thermal and mechanical properties of electrospun PMMA, PVC, Nylon 6, and Nylon 6,6.** Polymers for Advanced Technologies, v. 19, n. 2, p. 124–130, fev. 2008.

CHENG, X. et al. **Improving ultrafiltration membrane performance with pre-deposited carbon nanotubes/nanofibers layers for drinking water treatment.** Chemosphere, v. 234, p. 545–557, 1 nov. 2019.

CORRADINI, E. et al. **Preparation of Polymeric Mats Through Electrospinning for Technological Uses.** In: Recent Advances in Complex Functional Materials. Cham: Springer International Publishing, 2017. p. 83–128.

DELE-AFOLABI, T. T. et al. **Microstructure evolution and hardness of MWCNT-reinforced Sn-5Sb/Cu composite solder joints under different thermal aging conditions.** Microelectronics Reliability, v. 110, p. 113681, 1 jul. 2020.

ESCRIBÁ, A. et al. **Incorporation of nanomaterials on the electrospun membrane process with potential use in water treatment.** Colloids and Surfaces A: Physicochemical and Engineering Aspects, v. 624, p. 126775, 5 set. 2021.

GOGOI, A. et al. **Occurrence and fate of emerging contaminants in water environment: A review.** Groundwater for Sustainable Development, v. 6, n. December 2017, p. 169–180, 2018.

HE, Q. et al. **Excellent thermally conducting modified graphite nanoplatelets and MWCNTs/ poly(phenylene sulfone) composites for high-performance electromagnetic interference shielding effectiveness.** Composites Part A: Applied Science and Manufacturing, v. 143, n. January, p. 106280, 2021.

HEBBAR, R. S.; ISLOOR, A. M.; ISMAIL, A. F. **Contact Angle Measurements.** In: Membrane Characterization. [s.l.] Elsevier, 2017. p. 219–255.

HOUNGBO, G. F. **The United Nations world water development report 2018: Nature-Based Solutions for Water** (2018 Paris : UNESCO, Ed.)UNESCO Digital Library. Paris, France: [s.n.].

HU, G. et al. **Human health risk-based life cycle assessment of drinking water treatment for heavy metal(loids) removal.** Journal of Cleaner Production, v. 267, p. 121980, 2020.

HUANG, X. et al. **Performance enhancement of carbon nanotube/silicon solar cell by solution processable MoOx.** Applied Surface Science, v. 542, p. 148682, 15 mar. 2021.

HUTTON, G. **Global costs and benefits of reaching universal coverage of sanitation and drinking-water supply.** Journal of water and health, v. 11, n. 1, p. 1–12, mar. 2013.

HYLL, K. **Image-based quantitative infrared analysis and microparticle characterisation for pulp and paper applications.** [s.l: s.n.].

INKSON, B. J. **Scanning Electron Microscopy (SEM) and Transmission Electron Microscopy (TEM) for Materials Characterization.** In: Materials Characterization Using Nondestructive Evaluation (NDE) Methods. [s.l.] Elsevier

Inc., 2016. p. 17–43.

ISLAM, M. S.; MCCUTCHEON, J. R.; RAHAMAN, M. S. **A high flux polyvinyl acetate-coated electrospun nylon 6/SiO 2 composite microfiltration membrane for the separation of oil-in-water emulsion with improved antifouling performance.** Journal of Membrane Science, v. 537, n. February, p. 297–309, set. 2017.

JAIN, N.; JEE KANU, N. **The potential application of carbon nanotubes in water Treatment: A state-of-the-art-review.** Materials Today: Proceedings, 26 fev. 2021.

JAVIER, F.; MARTÍNEZ, M. **Modelización molecular de nanotubos de carbono Tesis Doctoral.** [s.l.] Granada University, 2010.

KARIIM, I. et al. **Development of MWCNTs/TiO2 nanoadsorbent for simultaneous removal of phenol and cyanide from refinery wastewater.** Scientific African, v. 10, p. e00593, 2020.

KAUR, S. et al. **Hot pressing of electrospun membrane composite and its influence on separation performance on thin film composite nanofiltration membrane.** Desalination, v. 279, n. 1–3, p. 201–209, set. 2011.

KHAN, D. et al. **Incorporation of carbon nanotubes in photoactive layer of organic solar cells.** Ain Shams Engineering Journal, 14 ago. 2020.

KING, R. P. **Non-Newtonian slurries.** In: Introduction to Practical Fluid Flow. [s.l.] Elsevier, 2002. p. 117–157.

KUMAR, M.; BORAH, P.; DEVI, P. **Priority and emerging pollutants in water.** In: Inorganic Pollutants in Water. [s.l.] Elsevier, 2020. p. 33–49.

LIU, Y. et al. **High-flux microfiltration filters based on electrospun polyvinylalcohol nanofibrous membranes.** Polymer, v. 54, n. 2, p. 548–556, jan.

2013.

LUAN, H.; TEYCHENE, B.; HUANG, H. **Efficient removal of As(III) by Cu nanoparticles intercalated in carbon nanotube membranes for drinking water treatment.** Chemical Engineering Journal, v. 355, p. 341–350, 1 jan. 2019.

MOFOKENG, M. et al. **Perflurooctyltriethoxy silane and carbon nanotubes-modified PVDF superoleophilic nanofibre membrane for oil-in-water adsorption and recovery.** Journal of Environmental Chemical Engineering, v. 8, n. 6, p. 104497, 1 dez. 2020.

MOHAMMADI, A. A. et al. **Adsorptive removal of endocrine disrupting compounds from aqueous solutions using magnetic multi-wall carbon nanotubes modified with chitosan biopolymer based on response surface methodology: Functionalization, kinetics, and isotherms studies.** International Journal of Biological Macromolecules, v. 155, p. 1019–1029, jul. 2020.

MULDER, M. **Basic Principles Of Membrane Technology.** Dordrecht ed. [s.l.] Springer, Dordrecht, 1996. v. 2

NAJAFI, V.; ABDOLLAHI, H. **Internally plasticized PVC by four different green plasticizer compounds.** European Polymer Journal, v. 128, n. March, 2020a.

NAJAFI, V.; ABDOLLAHI, H. **Internally plasticized PVC by four different green plasticizer compounds.** European Polymer Journal, v. 128, p. 109620, 5 abr. 2020b.

NGUYEN, J. N. T.; HARBISON, A. M. **Scanning electron microscopy sample preparation and imaging.** Methods in Molecular Biology, v. 1606, p. 71–84, 2017.

OSUNTOKUN, J.; AJIBADE, P. A. **Structural and Thermal Studies of ZnS and CdS Nanoparticles in Polymer Matrices.** Journal of Nanomaterials, v. 2016, n. January, 2016.

PARK, M. J. et al. **Hydrophilic polyvinyl alcohol coating on hydrophobic electrospun nanofiber membrane for high performance thin film composite forward osmosis membrane.** Desalination, v. 426, n. October 2017, p. 50–59, jan. 2018.

PARREIRA, L. S. et al. **MWCNT-COOH supported PtSnNi electrocatalysts for direct ethanol fuel cells: Low Pt content, selectivity and chemical stability.** Renewable Energy, v. 143, p. 1397–1405, 2019.

QUOC PHAM, L. et al. **A Review on Electrospun PVC Nanofibers: Fabrication, Properties, and Application.** Fibers, v. 9, n. 2, p. 12, 3 fev. 2021.

RAHMATI, M. et al. **Electrospinning for tissue engineering applications.** Progress in Materials Science, v. 117, n. July, p. 100721, abr. 2021.

RIBEIRO, B. et al. **Carbon nanotube buckypaper reinforced polymer composites: A review.** Polimeros, v. 27, n. 3, p. 247–255, 2017.

RILES, E.; BROOK, R. **The Air Quality Index: A Tool for Managing Patients with Cardiopulmonary Disease.** The American Journal of Medicine, v. 124, n. 8, p. 705–707, 1 ago. 2011.

SHEN, K. et al. **Salt-tuned fabrication of novel polyamide composite nanofiltration membranes with three-dimensional turing structures for effective desalination.** Journal of Membrane Science, v. 607, n. February, p. 118153, jul. 2020.

STACE, E. T. et al. **Biomaterials: Electrospinning.** Third Edit ed. [s.l.] Elsevier, 2019. v. 5

SUJA, P. S. et al. **Electrospun Nanofibrous Membranes for Water Purification.** Polymer Reviews, v. 57, n. 3, p. 467–504, 3 jul. 2017.

SUMIO LIJIMA. © 19 9 1 **Nature Publishing Group** 그라첼꺼. Nature, v. 354,

p. 56–58, 1991.

THIRUGNANASAMBANTHAM, K. G. et al. **A comprehensive review: Influence of the concentration of carbon nanotubes (CNT) on mechanical characteristics of aluminium metal matrix composites: Part 1**. Materials Today: Proceedings, 2 jan. 2021.

TIWARI, S. K.; VENKATRAMAN, S. S. **Importance of viscosity parameters in electrospinning : Of monolithic and core – shell fi bers.** Materials Science & Engineering C, v. 32, n. 5, p. 1037–1042, 2012.

ULBRICHT, M. **Advanced functional polymer membranes.** Polymer, v. 47, n. 7, p. 2217–2262, mar. 2006.

WADA, Y. et al. **Modeling global water use for the 21st century: the Water Futures and Solutions (WFaS) initiative and its approaches.** Geoscientific Model Development, v. 9, n. 1, p. 175–222, 21 jan. 2016.

WANG, Z. et al. **Hot-pressed PAN/PVDF hybrid electrospun nanofiber membranes for ultrafiltration.** Journal of Membrane Science, v. 611, n. May, p. 118327, out. 2020.

WEN, Q. et al. **Flexible inorganic nanofibrous membranes with hierarchical porosity for efficient water purification.** Chemical Science, v. 4, n. 12, p. 4378, 2013a.

WEN, Q. et al. **Flexible inorganic nanofibrous membranes with hierarchical porosity for efficient water purification.** Chemical Science, v. 4, n. 12, p. 4378–4382, 2013b.

WWDR, 2015. **The United Nations world water development report 2015: water for a sustainable world.** UNESCO Publishing, Paris. [s.l: s.n.].

WYPYCH, G. **PVC poly(vinyl chloride).** In: Handbook of Polymers. [s.l.] Elsevier, 2016a. v. 59p. 618–624.

WYPYCH, G. **PVC poly(vinyl chloride).** In: Handbook of Polymers. [s.l.] Elsevier, 2016b. p. 618–624.

WYPYCH, G. **PVC MANUFACTURE TECHNOLOGY.** In: PVC Degradation and Stabilization. [s.l.] Elsevier, 2020. p. 25–46.

XIE, R.; SUGIME, H.; NODA, S. **High-performance solution-based silicon heterojunction solar cells using carbon nanotube with polymeric acid doping.** Carbon, v. 175, p. 519–524, 30 abr. 2021.

YADAV, S. et al. **Recent developments in forward osmosis membranes using carbon-based nanomaterials.** Desalination, v. 482, n. January, p. 114375, maio 2020.

YIP, N. Y. et al. **High Performance Thin-Film Composite Forward Osmosis Membrane.** Environmental Science & Technology, v. 44, n. 10, p. 3812–3818, 15 maio 2010.

ZHANG, Y. et al. **Enhanced photodegradability of PVC plastics film by codoping nano-graphite and TiO2.** Polymer Degradation and Stability, v. 181, p. 109332, 2020a.

ZHANG, Y. et al. **Nanofiber composite forward osmosis (NCFO) membranes for enhanced antibiotics rejection: Fabrication, performance, mechanism, and simulation.** Journal of Membrane Science, v. 595, n. August 2019, p. 117425, fev. 2020b.

ZHAO, Z. et al. **High performance ultrafiltration membrane based on modified chitosan coating and electrospun nanofibrous PVDF scaffolds.** Journal of Membrane Science, v. 394–395, p. 209–217, mar. 2012.